

# EFFECTIVE LOCAL ANHARMONIC POTENTIALS IN SOLIDS. A MODEL APPROACH

I.V. STASYUK, YU.V. SIZONENKO

*Institute for Condensed Matter Physics  
of the Ukrainian National Academy of Sciences  
1 Svientsitskii St., UA-290011 Lviv, Ukraine*

Received May 15, 1995

The role of electron-phonon interaction in the formation of local anharmonic lattice potentials in crystal is investigated on the basis of the simple model. The case of three particle ion cluster  $A - B - A$  is considered. The interaction of the electron subsystem with the vibrational modes  $u_r$  and  $u_{ir}$ , being Raman and infrared-active respectively, is taken into account. The calculation of effective ion potentials and distribution functions is performed. The possibility of realization of one  $(u_r^0, 0)$  or two  $(u_r^0, \pm u_{ir}^0)$  equilibrium positions of cluster at various values of the theory parameters, electron concentration and temperature is discussed. The "phase" diagrams are built for the description of possible states of the cluster and of the corresponding topological types of effective potentials. The energy spectrum of the model is analyzed. It is shown, that the quazipolaron effect leads to the formation of doublet in the low frequency range. The sublevel distance is defined by the electron-transfer parameter renormalized due to electron-phonon coupling.

## 1. Introduction

The investigation of quasi-one-dimensional systems with the local anharmonicity is of great interest for study of ionic or crystalline systems, where particles of some kind are moving in effective field characterized by double-well potential. Such objects can be represented by H-bonded crystals or complexes with anharmonic proton motion. Another example of such systems are high temperature superconducting crystals of YBaCuO type, where chain structures consisting of O and Cu ions are observed and oxygen ion motion possesses strong anharmonicity. The vibrations of the so-called apex oxygen ions have the same property in such systems [1-3].

Results of the quantum ab initio calculations performed for molecular complexes with H-bonds show that the form of the adiabatical potential of the proton on H-bond depends on the distance between external ions  $R_{A-A'}$  [4-6]. Two-minima potential is typical for the distances larger then critical one. For the smaller values of distance  $R_{A-A'}$  only one minimum is observed.

It must be pointed out that the potential sensitivity to the distance  $R_{A-A'}$  shows the strong electron-phonon coupling, so one can doubt in fitting of the adiabatic approximation. Effective potential for the particle B on the bond  $A - B - A'$  must be formed self-consistently and possesses

statistical nature, being dependent on the temperature. The problem of the investigation of such potentials can be solved on the base of quantum chemical calculations; it can be solved also using rather simple models.

Model which can be used in our approach was proposed in [1,7] for the description of the O-Cu-O clusters in the YBaCuO crystals. The Hamiltonian of the cluster written in the strong coupling approximation includes electron transfer as well as electron interaction with the vibrational modes (as in Holstein model [8], only terms diagonal on the electron variables were taken into account). Anharmonicity is absent in the initial phonon Hamiltonian. It was shown that anharmonicity may appear due to sufficiently strong electron-phonon interaction. The central ion distribution function possesses in this case two equivalent maxima reflecting the existence of two displaced equilibrium positions.

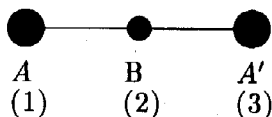
The idea of polaron nature (as the result of electron-phonon interaction) of the anharmonicity of the vibrations of O-Cu-O complexes or apex oxygen ions alone in YBaCuO-type crystals was declared also in [9,10]. In the frame of the Holstein model the influence of the electron-electron interaction and antiferromagnetic spin correlations on the polaron anharmonicity was examined in [9]. Effective electron correlations that appear due to the electron-phonon coupling were studied in [11] in the case of neglecting of the direct Hubbard interaction. Papers [10,12] were devoted to the construction of the effective electron Hamiltonian and to the analysis of the possibilities of the superconducting electron pairing on the basis of the Holstein-Hubbard model and some its generalizations.

However, a set of problems connected with appearance of the locally anharmonic lattice potentials needs a more detailed study. The thermodynamical criteria of the formation of such potentials as well as the role of the Coulomb components of the interactions between excessive charges, which appear during the displacements of ions and electron redistribution are not studied yet. The peculiarities of electron and vibrational spectra of the crystal systems and clusters, where the local anharmonicity of the vibrations is caused by the above mentioned quasipolaron effect also are not investigated (only simple approximations were applied).

In the present paper we will examine these problems, using and generalizing the simple model of 3-ion cluster proposed in [7]. We will perform statistical averaging over the states of electron subsystem and investigate the equilibrium states and configurations of the complex, being based on the condition of the corresponding thermodynamic potential minimum. The possibility of the different charge states of cluster caused by the change of mean number of the electrons on the cluster will be taken into account. The evaluation of the distribution function over the ions coordinates will be done and the criteria of the appearance of the local anharmonicity in the effective potential at the presence of the Coulomb parts of the electron-electron and electron-ion interactions will be obtained. We will also investigate the peculiarities of the energy spectrum caused by the mixing of the modes due to the electron transfer.

## 2. Model Hamiltonian

Symmetrical ion cluster  $A - B - A'$



is considered as an element of a crystal structure. The potential energy of such cluster can be written in the harmonical approximation in the diagonal form

$$U = k_r \frac{u_r^2}{2} + k_{ir} \frac{u_{ir}^2}{2} + k_f \frac{u_f^2}{2}, \quad (2.1)$$

here normal coordinates  $u_r, u_{ir}, u_f$  depend on the ions displacements  $w_i$  from the initial equilibrium positions

$$\begin{aligned} u_r &= \sqrt{\frac{m}{2}}(w_3 - w_1); \\ u_{ir} &= \sqrt{\frac{mm'}{2M}}(w_1 + w_3 - 2w_2); \\ u_f &= \frac{m}{\sqrt{M}}(w_1 + w_3 + \frac{m'}{m}w_2); \\ M &= 2m + m'; \\ (m_1 = m_3 = m; & \quad m_2 = m'); \end{aligned} \quad (2.2)$$

$u_r$  describes mutual displacements of external ions; corresponding vibrations can be observed in the experiments on the Raman scattering.  $u_{ir}$  determines the displacement of the central ion from the centre of mass of the external ions; such type vibrations are manifested in IR spectrum.  $u_f$  describes displacement of the centre of mass of complex (in the case of free complex  $k_f = 0$ ).

With the help of the phonon creation and annihilation operators

$$u_i = \frac{1}{\sqrt{m}} \sqrt{\frac{\hbar}{2\omega_i}} (b_i + b_i^\dagger); \quad \omega_i = \sqrt{\frac{k_i}{m}} \quad (i = r, ir) \quad (2.3)$$

the phonon Hamiltonian can be represented in the standard form (operator of the kinetic energy is also included here)

$$H_{ph} = \sum_i \hbar\omega_i (b_i^\dagger b_i + 1/2). \quad (2.4)$$

Electronic part of the Hamiltonian can be written in the second quantization form on the basis of wave functions of valence electrons localized on the separate ions. Taking into account only one orbitally nondegenerated state for each ion (as it was done in [7]) and considering electron transfer, Coulomb interaction between ions ( $U$  and  $U'$ ) and Hubbard type Coulomb correlation ( $A$  and  $A'$ ) we can obtain:

$$\begin{aligned} H_{el} &= \sum_i \epsilon_i n_i + U(n_1 + n_3)n_2 + U'n_1n_3 + \\ &+ A(n_{1\uparrow}n_{1\downarrow} + n_{3\uparrow}n_{3\downarrow}) + A'n_{2\uparrow}n_{2\downarrow} + \\ &+ t \sum_{\sigma} (a_{1\sigma}^\dagger a_{2\sigma} + a_{2\sigma}^\dagger a_{1\sigma} + a_{2\sigma}^\dagger a_{3\sigma} + a_{3\sigma}^\dagger a_{2\sigma}). \end{aligned} \quad (2.5)$$

Here  $\epsilon_i$  are the energies of corresponding localized states ( $\epsilon_1 = \epsilon_3 \neq \epsilon_2; n_i = \sum_{\sigma} n_{i\sigma}$ ). After the separating of the electrostatic components of the internal fields

$$\begin{aligned} \epsilon_1 &= \epsilon_1^0 - \frac{e^2}{d} z_2 - \frac{e^2}{2d} z_1; \\ \epsilon_2 &= \epsilon_2^0 - \frac{2e^2}{d} z_1; \end{aligned} \quad (2.6)$$

$U = \frac{e^2}{d}$ ;  $U' = \frac{e^2}{2d}$  ( $z_i e$  are charges of ions (excluding valence electrons);  $z_1 = z_3$ ,  $2d$  is distance between ions A and A').

The interaction between electron and phonon subsystems can be obtained when the dependence of the parameters  $\epsilon_i$ ,  $t$ ,  $U$  and  $U'$  on the ion coordinates is taken into consideration. In the linear on the ion displacements approximation equalities hold:

$$\begin{aligned} \epsilon_1 &\rightarrow \epsilon_1 - \gamma(w_2 - w_1) - \beta(w_3 - w_1); \\ \epsilon_3 &\rightarrow \epsilon_1 - \gamma(w_3 - w_2) - \beta(w_3 - w_1); \\ \epsilon_2 &\rightarrow \epsilon_2 + \gamma'(w_3 - w_1); \\ U(1, 2) &= U - \bar{\alpha}(w_2 - w_1); \\ U(2, 3) &= U - \bar{\alpha}(w_3 - w_2); \\ U(1, 3) &= U' - \bar{\beta}(w_3 - w_1), \end{aligned} \quad (2.7)$$

where

$$\begin{aligned} \gamma &= \gamma_0 - \frac{e^2}{d^2} z_2; & \gamma' &= \gamma'_0 + \frac{e^2}{d^2} z_1; \\ \beta &= -\frac{e^2}{4d^2} z_1; & \bar{\alpha} &= \frac{e^2}{d^2}; \\ \bar{\beta} &= \frac{e^2}{4d^2}, \end{aligned} \quad (2.8)$$

here  $\gamma_0, \gamma'_0$  being short range components of coupling constants. Similarly,

$$\begin{aligned} t(1, 2) &= t - \delta(w_2 - w_1); \\ t(2, 3) &= t - \delta(w_3 - w_2). \end{aligned} \quad (2.9)$$

After transition to the normal coordinates the following Hamiltonian of the electron-phonon interaction in the cluster can be obtained

$$\begin{aligned} H_{el-ph} &= \left[ \frac{1}{\sqrt{2}}(\gamma + 2\beta)(n_1 + n_3) - \sqrt{2}\gamma'n_2 + \right. \\ &\quad \left. + \frac{1}{\sqrt{2}}\bar{\alpha}n_2(n_1 + n_3) + \sqrt{2}\beta n_1 n_3 \right] u_r - \\ &\quad - [\gamma(n_1 - n_3) + \bar{\alpha}n_2(n_1 - n_3)] \sqrt{\frac{M}{2m'}} u_{ir} + \\ &\quad + \delta \sum_{\sigma} (a_{1\sigma}^+ a_{2\sigma} + a_{2\sigma}^+ a_{1\sigma} + a_{2\sigma}^+ a_{3\sigma} + a_{3\sigma}^+ a_{2\sigma}) \frac{1}{\sqrt{2}} u_r - \\ &\quad - \delta \sum_{\sigma} (a_{1\sigma}^+ a_{2\sigma} + a_{2\sigma}^+ a_{1\sigma} - a_{2\sigma}^+ a_{3\sigma} - a_{3\sigma}^+ a_{2\sigma}) \sqrt{\frac{M}{2m'}} u_{ir} \end{aligned} \quad (2.10)$$

(we consider only the interactions with optical modes  $u_r$  and  $u_{ir}$ ).

In the adopted approximation, the full cluster Hamiltonian consists of parts (2.4), (2.5) and (2.10):

$$H = H_{ph} + H_{el} + H_{el-ph}. \quad (2.11)$$

In comparison with the energy operator, which was used in [7], here, in addition, we have the modulations of electron interaction parameters and transfer integral at the displacements of ions.

### 3. Distribution function and effective potential energy of ion subsystem

Our first step will be to obtain and to investigate the potential energy of ion subsystem of the cluster as a function of ion coordinates (or normal coordinates  $u_r$  and  $u_{ir}$ ).

Minima of the "conditional" free energy  $F|_{u_r, u_{ir}}$  (in the case of fixed number of electrons in cluster  $N$ )<sup>1</sup> or "conditional" thermodynamic potential  $\Phi|_{u_r, u_{ir}, \mu}$  (in the case of the fixed value of the chemical potential) determine equilibrium cluster configurations. Distribution function over the normal coordinates is connected with the above mentioned thermodynamical characteristics:

$$f(x, y) = \langle \delta(x - u_r) \delta(y - u_{ir}) \rangle. \quad (3.1)$$

The averaging is performed here over the statistical distribution with the Hamiltonian (2.11). Calculating the  $F$ ,  $\Phi$  and  $f$  functions we examine below some particular cases and study the role of different components of electron-phonon interaction.

#### 3.1. Classical approximation

First of all let us analyse the results obtained in the classical approximation (assuming that the normal coordinates are classical variables and neglecting their noncommutativity with corresponding momentum operators). Such assumption allows to diagonalize the electronic part of the Hamiltonian.

In the simplified case (which was considered in [1,7]) when the interaction between electrons was neglected, electron-phonon interaction was written in the form

$$H_{el-ph}^0 = -\Lambda_r u_r (n_1 + n_3 - 2n_2) - \Lambda_{ir} u_{ir} (n_3 - n_1) \quad (3.2)$$

(this corresponds to the Holstein model [8]) and spin degrees of freedom were not considered, the electron Hamiltonian

$$H = \sum_{i=1}^3 \epsilon_i a_i^\dagger a_i + t(a_1^\dagger a_2 + a_2^\dagger a_1 + a_2^\dagger a_3 + a_3^\dagger a_2) - \Lambda_r u_r (n_1 + n_3 - 2n_2) - \Lambda_{ir} u_{ir} (n_3 - n_1) \quad (3.3)$$

can be rewritten in the diagonal form using the unitary transformation  $a_i = \sum_j W_{ij}^{-1} c_j$  to the new Fermi-operators:

$$H = \sum_{i=1}^3 \tilde{\epsilon}_i c_i^\dagger c_i + k_r \frac{u_r^2}{2} + k_{ir} \frac{u_{ir}^2}{2} + K, \quad (3.4)$$

where  $K$  is operator of ion kinetic energy. Energies  $\tilde{\epsilon}_i$  are the functions of  $u_r$  and  $u_{ir}$ .

$$\begin{aligned} \tilde{\epsilon}_1 &= \epsilon_1 - \Lambda_r u_r + \Lambda_{ir} u_{ir}; \\ \tilde{\epsilon}_2 &= \epsilon_2 + 2\Lambda_r u_r; \\ \tilde{\epsilon}_3 &= \epsilon_1 - \Lambda_r u_r - \Lambda_{ir} u_{ir}; \end{aligned} \quad (3.5)$$

<sup>1</sup>See Appendix 1

Effective thermodynamic potential  $\Xi(u_r, u_{ir})$  after the averaging over the electron degrees of freedom

$$\Xi(u_r, u_{ir}) = Sp_{(el)}\{\exp[-\beta(H - \mu N)]\} \quad (3.6)$$

and extracting its coordinate part is equal to

$$\Xi(u_r, u_{ir}) = \exp\left[-\frac{\beta}{2}(k_r u_r^2 + k_{ir} u_{ir}^2)\right] \prod_i [1 + e^{-\beta(\bar{\epsilon}_i - \mu)}]. \quad (3.7)$$

At the fixed average number of electron in cluster, the chemical potential can be found from the relation:

$$\sum_i \frac{1}{e^{\beta(\bar{\epsilon}_i - \mu)} + 1} = N; \quad 0 \leq N \leq 3. \quad (3.8)$$

The equilibrium state in this case corresponds to the minimum of free energy

$$\begin{aligned} F(u_r, u_{ir}) &= \Phi(u_r, u_{ir}) + \mu(u_r, u_{ir})N; \\ \Phi(u_r, u_{ir}) &= -\theta \ln \Xi(u_r, u_{ir}), \end{aligned} \quad (3.9)$$

and function  $F(u_r, u_{ir})$  has the meaning of effective potential energy.

Problem of evaluation of the chemical potential  $\mu(u_r, u_{ir})$  and, respectively, of the function  $F$  can be solved analytically at  $t = 0$  in the limit of the absolute zero temperature. Since the initial Hamiltonian has diagonal form, the chemical potential can be easily calculated. Its dependence on the average number of electrons  $N$  is shown in Fig.1. The investigation of the free energy profiles on the plane  $(u_r, u_{ir})$  for the different values of  $N$  shows that single minimum of function  $(u_r^0, 0)$  as well as double symmetric minima  $(u_r^{0'}, \pm u_{ir}^{0'})$  [13] can be observed. Obtained results are presented in the following tables.

	Coordinates of minima		
$0 \leq N \leq 1$	$(-\frac{2\Delta_r}{k_r} N, 0)$		(A.1)
(A)	$(\frac{2\Delta_r}{k_r} N, \pm \frac{\Delta_{ir}}{k_{ir}} N)$		(A.2)
$1 \leq N \leq 2$	$(-\frac{\Delta_r}{k_r} (3 - N), \pm \frac{\Delta_{ir}}{k_{ir}} (N - 1))$		(B.1)
(B)	$(\frac{\Delta_r}{k_r} (3 - 2N), \pm \frac{\Delta_{ir}}{k_{ir}})$		(B.2)
	$(\frac{\Delta_r}{k_r} N, \pm \frac{\Delta_{ir}}{k_{ir}} (2 - N))$		(B.3)
$2 \leq N \leq 3$	$(-\frac{\Delta_r}{k_r} (2 - N), \pm \frac{\Delta_{ir}}{k_{ir}} (2 - N))$		(C.1)
(C)	$(\frac{2\Delta_r}{k_r} (2 - N), 0)$		(C.2)

	Conditions of minima realization		
	$\epsilon_2 - \epsilon_1 < \frac{6\Delta_r^2}{k_r}$		(A.1)
(A)	$\epsilon_2 - \epsilon_1 > -\frac{3\Delta_r^2}{k_r} N - \frac{\Delta_{ir}^2}{k_{ir}} N$		(A.2)
	$\epsilon_2 - \epsilon_1 < \frac{3\Delta_r^2}{k_r} (3 - N) - \frac{\Delta_{ir}^2}{k_{ir}} (N - 1)$		(B.1)
(B)	$-\frac{3\Delta_r^2}{k_r} (3 - 2N) - \frac{\Delta_{ir}^2}{k_{ir}} < \epsilon_2 - \epsilon_1 < -\frac{3\Delta_r^2}{k_r} (3 - 2N) + \frac{\Delta_{ir}^2}{k_{ir}}$		(B.2)
	$\epsilon_2 - \epsilon_1 > -\frac{3\Delta_r^2}{k_r} N + \frac{\Delta_{ir}^2}{k_{ir}} (2 - N)$		(B.3)
	$\epsilon_2 - \epsilon_1 < -\frac{3\Delta_r^2}{k_r} (2 - N) - \frac{\Delta_{ir}^2}{k_{ir}} (2 - N)$		(C.1)
(C)	$\epsilon_2 - \epsilon_1 > -\frac{6\Delta_r^2}{k_r} (2 - N)$		(C.2)

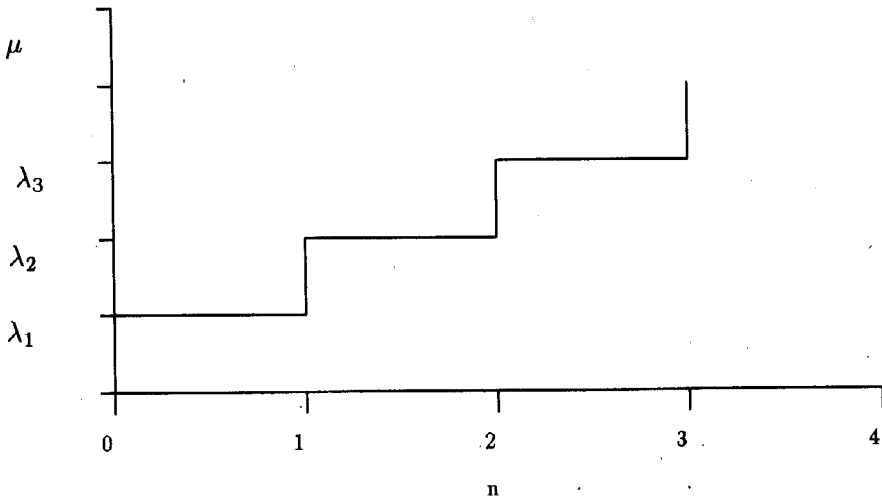


Figure 1. The dependence of the chemical potential on the electron number for the model with Hamiltonian (3.4). Values of parameters  $\lambda_1$  are taken from the set  $(\tilde{\epsilon}_1, \tilde{\epsilon}_2, \tilde{\epsilon}_3)$  using the rule  $\lambda_1 < \lambda_2 < \lambda_3$ .

As one can see in the cases  $(0 \leq N \leq 1)$  and  $(2 \leq N \leq 3)$  there is a possibility of simultaneous existence of the double minimum and a single one. Conditions of their coexistence can be obtained from nonequalities (A.1), (A.2) and (C.1), (C.2).

Similar analysis of effective potential energy profiles was also performed in the case  $\mu = \text{const}$  [13]. In this case equilibrium configurations of the complex are determined by the function  $\Phi(u_r, u_{ir})$ . When  $\beta \rightarrow 0, t = 0$

$$\Phi = \Phi' + k_r \frac{u_r^2}{2} + k_{ir} \frac{u_{ir}^2}{2}, \tag{3.10}$$

here

$$\Phi' = -\theta \sum_i \ln(1 + e^{-\beta(\lambda_i - \mu)}) \rightarrow_{T \rightarrow 0} \sum_{\lambda_i < \mu} (\lambda_i - \mu). \tag{3.11}$$

$\Phi' = 0$  when  $\mu < \min(\lambda_1, \lambda_2)$ ;  $\Phi' = 2\epsilon_1 - \epsilon_2 - 3\mu$  when  $\mu < \max(\lambda_1, \lambda_2)$ ; in both cases function  $\Phi$  possesses minimum at the point (0;0). The analysis of other variants, done in [13], shows, that as in the case of  $N = \text{const}$  minima (single as well as double ones) do exist in the other points; in some ranges of chemical potential  $\mu$  value they can occur simultaneously.

At the nonzero values of transfer parameter  $t$  and at nonzero temperature the effective potential ( $F$  or  $\Phi$  function) profiles were calculated numerically.

Obtained graphs are shown on Fig.2,3. Free energy profiles at the different values of electron number  $N$ , temperature  $T$ , transfer parameter  $t$  and energy values  $\epsilon_1, \epsilon_2$  are presented in Fig. 2. In the case  $0 < N < 1$  the change of the sign of the difference  $\epsilon_1 - \epsilon_2$  leads to the replacement of the double minima (Fig. 2.1) by the single one (Fig. 2.2) with the simultaneous change of  $u_r$  sign, and at  $1 < N < 2$  we can observe double minima independently on sign of the the difference  $\epsilon_1 - \epsilon_2$ . Variation of electron

number  $N$  within mentioned intervals doesn't change profiles qualitatively, but at  $0 < N < 1$  increase of  $N$  results in increasing of the distance between minima (in the case of double minima  $F$ ), and at  $1 < N < 2$  the influence of change of  $N$  has opposite character (Fig. 2.5, 2.6).

The barrier height between minima of the function  $F$  decreases with temperature and increases with the increase of the transfer parameter  $t$  (Fig. 2.3, 2.4). At the rather high temperatures minima can join together into one.

The specific situation takes place in the case of close values of energies  $\epsilon_1, \epsilon_2$ . As it is shown by Fig. 2.7, 2.8 at  $0 < N < 1$  double minima of function  $F$  as well as the single one can coexist when conditions given in the table are satisfied. The relation between their minima depths depends on the  $\epsilon_1, \epsilon_2$  values. At  $1 < N < 2$  the tendency to appearance of the additional minima besides the initial one can be observed while the  $\epsilon_i$  values are coming nearer one to another [13].

The behaviour of the thermodynamical potential  $\Omega$  in the  $(u_r, u_{ir})$  plane at the different values of chemical potential  $\mu$  is presented at Fig. 3. At the chemical potential values, smaller than  $\min(\epsilon_1, \epsilon_2)$  or greater than  $\max(\epsilon_1, \epsilon_2)$ , function  $\Omega$  possesses central minimum at the point  $(0,0)$ . In addition, in the first case at the increase of  $\mu$  the double minimum gradually appears and becomes then the main one. At the further increase of the chemical potential new single minimum appears (with coordinate  $u_r \neq 0$ ); this minimum disappears at the large positive values of chemical potential  $\mu$  (see [13]). There are some ranges of chemical potential values where thermodynamic potential  $\Omega$  possesses single and double minima simultaneously (Fig. 3.3) or two single minima with coordinate  $u_{ir} = 0$  (Fig. 3.4).

The illustrations given above confirm the analytical results concerning the conditions of the occurrence of double or single minima of functions  $F$  and  $\Omega$ .

Values of parameters used for evaluation of the free energy profiles presented at Fig. 2.6 are close to the ones used in [7] for the constructing of the distribution function over the  $u_{ir}$  coordinate for the complex O-Cu-O in the  $YBaCuO$  crystal. Double minima character of the potential in our case is in a good agreement with the existence of the double maximum of the distribution function obtained in [7].

Some quantitative difference is connected with the neglecting here the spin degeneracy and Hubbard electron correlation, also it can be caused by the using of classical approximation in the description of ion vibration.

### 3.2. Quantum description of the vibrations (the case of zero transfer).

Let us examine now the problem of evaluation of the distribution function  $f(x, y)$  over the ion coordinates in the quantum case. We shall use the simplified model, described in item 3.1. Passing to the quantum description of the vibrations we shall restrict ourselves to the case  $t = 0$ .<sup>2</sup>

Hamiltonian in this approximation has the form

$$\hat{H} = \sum_i \epsilon_i n_i + \sum_{k=1}^2 \hbar \omega_k b_k^+ b_k - \Lambda_1 (n_1 + n_3 - 2n_2) \sqrt{\frac{\hbar}{2m\omega_1}} (b_1 + b_1^+) - \Lambda_{ir} (n_3 - n_1) \sqrt{\frac{\hbar}{2m\omega_2}} (b_2 + b_2^+) \quad (3.12)$$

<sup>2</sup>Exact solution of the Hubbard-Holstein model in the zero-bandwidth limit in the case of interactions with one branch of the lattice vibrations was given in [14,15]



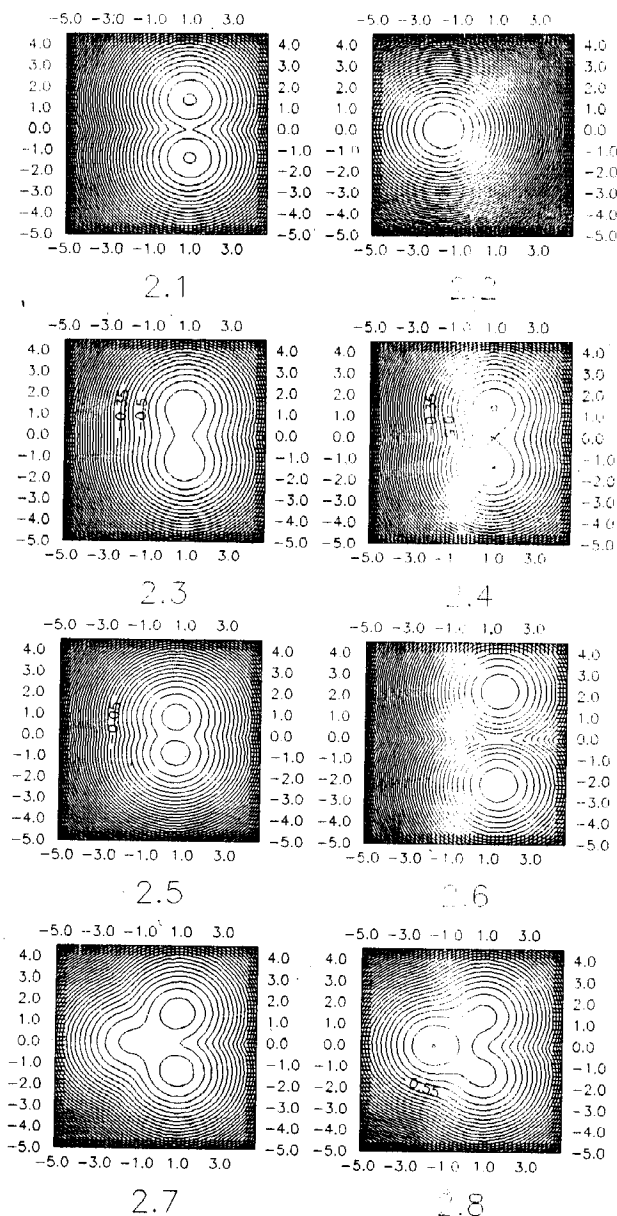


Figure 2. The profiles of free energy (the values of parameters correspond to the O-Cu-O cluster in YBaCuO crystal); classical approximation.  $\Lambda_r = 16$ ;  $\Lambda_{ir} = 7$ ;

2.1	$\epsilon_1 = -1.0,$	$\epsilon_2 = 1.0,$	$t = 0.1,$	$T = 0.014$	$n = 0.5$
2.2	$\epsilon_1 = 1.0,$	$\epsilon_2 = -1.0,$	$t = 0.1,$	$T = 0.014$	$n = 0.5$
2.3	$\epsilon_1 = -1.0,$	$\epsilon_2 = 1.0,$	$t = 0.5,$	$T = 0.014$	$n = 0.5$
2.4	$\epsilon_1 = -1.0,$	$\epsilon_2 = 1.0,$	$t = 0.1,$	$T = 1.4$	$n = 0.5$
2.5	$\epsilon_1 = -1.0,$	$\epsilon_2 = 1.0,$	$t = 0.1,$	$T = 0.014$	$n = 0.3$
2.6	$\epsilon_1 = -1.0,$	$\epsilon_2 = 1.0,$	$t = 0.1,$	$T = 0.014$	$n = 0.8$
2.7	$\epsilon_1 = 0.9,$	$\epsilon_2 = 1.0,$	$t = 0.1,$	$T = 0.014$	$n = 0.5$
2.8	$\epsilon_1 = 1.1,$	$\epsilon_2 = 1.0,$	$t = 0.1,$	$T = 0.014$	$n = 0.5$

The following dimensionless parameters are used:

$u_\alpha \rightarrow u_\alpha / \sqrt{\hbar/\omega_\alpha}$ ;  $\Lambda_\alpha \rightarrow \Lambda_\alpha / \sqrt{\hbar/\omega_\alpha} (\hbar\omega_\alpha)$ ;  $T \rightarrow kT / (\hbar/\omega_r)$ . The quantities  $\epsilon_1, \epsilon_2, t$  and  $F$  are given in eV. Energy distances between the lines in figures are 0.03 eV.

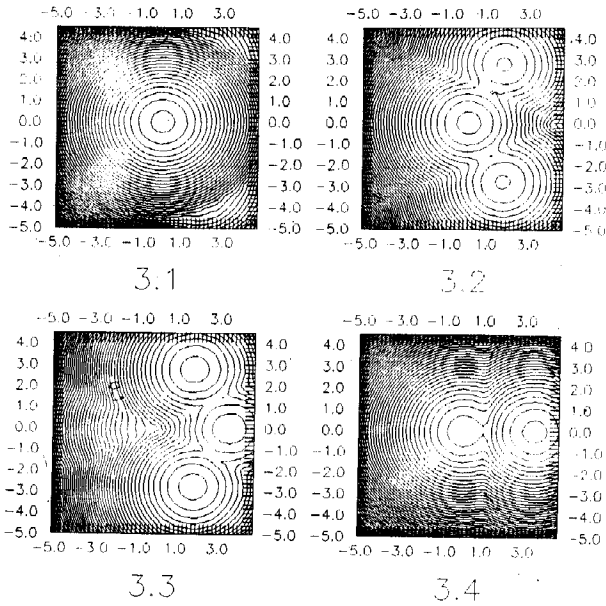


Figure 3. The profiles of thermodynamical potential  $\Omega$ ; classical approximation.  $\Lambda_r = 16$ ;  $\Lambda_{ir} = 7$ ;  $t = 0.1$ ,  $T = 0.014$ ,  $\epsilon_1 = -1.0$ ,  $\epsilon_2 = 1.0$ .  
 3.1  $\mu = -2.0$  3.2  $\mu = -1.4$  3.3  $\mu = -1.0$  3.4  $\mu = 1.2$

(indices 1,2 at the phonon operators correspond to the  $r$  and  $ir$  modes).

Due to the commutativity of the operator multipliers at  $(b_i + b_i^+)$  with the electron part of the Hamiltonian, we can separate phonon and electron variables with the help of the displacement Holstein-Lang-Firsov transformation [8,16]

$$\hat{H} \rightarrow \tilde{H} = e^{\hat{S}} \hat{H} e^{-\hat{S}}, \quad (3.13)$$

where

$$\hat{S} = \sum_{k=1}^2 \alpha_k (b_k - b_k^+); \quad (3.14)$$

$$\begin{aligned} \alpha_1 &= \sqrt{\frac{\hbar}{2m\omega_1}} \frac{\Lambda_1}{\hbar\omega_1} (n_1 + n_3 - 2n_2); \\ \alpha_2 &= \sqrt{\frac{\hbar}{2m\omega_2}} \frac{\Lambda_2}{\hbar\omega_2} (n_3 - n_1). \end{aligned} \quad (3.15)$$

Here

$$\begin{aligned} e^{\hat{S}} n_i e^{-\hat{S}} &= n_i; \\ e^{\hat{S}} b_i e^{-\hat{S}} &= b_i + \alpha_i. \end{aligned} \quad (3.16)$$

Such transformation can be represented as the transition to new operators

$$b_i = \tilde{b}_i + \alpha_i, \quad (3.17)$$

describing vibrations with respect to new equilibrium positions depending on the electron states occupation. The transformed Hamiltonian can be written as

$$\hat{H} = (\epsilon_1 - \varphi_1 - \varphi_2)(n_1 + n_3) + (\epsilon_2 - 4\varphi_1)n_2 + 2(\varphi_2 - \varphi_1)n_1n_3 + 4\varphi_1(n_1 + n_3)n_2 + \sum_{r=1}^2 \hbar\omega_r \tilde{b}_r^+ \tilde{b}_r, \quad (3.18)$$

where

$$\varphi_r = \frac{\Lambda_r^2}{2m\omega_r^2}. \quad (3.19)$$

Using the basis  $|n_1 n_2 n_3\rangle$  of the electron states

$$\begin{aligned} |000\rangle &= |1\rangle & |110\rangle &= |5\rangle \\ |100\rangle &= |2\rangle & |101\rangle &= |6\rangle \\ |010\rangle &= |3\rangle & |011\rangle &= |7\rangle \\ |001\rangle &= |4\rangle & |111\rangle &= |8\rangle \end{aligned} \quad (3.20)$$

we introduce Hubbard operators  $X^{pq} = |p\rangle\langle q|$ . In this representation

$$\begin{aligned} n_1 &= X^{22} + X^{55} + X^{66} + X^{88}, \\ n_2 &= X^{33} + X^{55} + X^{77} + X^{88}, \\ n_3 &= X^{44} + X^{66} + X^{77} + X^{88} \end{aligned} \quad (3.21)$$

and Hamiltonian  $\hat{H}$  has the diagonal form

$$\hat{H} = \sum_p \lambda_p X^{pp} + \sum_{r=1}^2 \hbar\omega_r \tilde{b}_r^+ \tilde{b}_r. \quad (3.22)$$

Here

$$\begin{aligned} \lambda_1 &= 0; & \lambda_2 &= \lambda_4 = \epsilon_1 - \varphi_1 - \varphi_2; \\ \lambda_3 &= \epsilon_2 - 4\varphi_1; & \lambda_5 &= \lambda_7 = \epsilon_1 + \epsilon_2 - \varphi_1 - \varphi_2; \\ \lambda_6 &= 2\epsilon_1 - 4\varphi_1; & \lambda_8 &= 2\epsilon_1 + \epsilon_2. \end{aligned} \quad (3.23)$$

Let us evaluate function  $f(x, y)$  for the system described by the Hamiltonian (3.22). We are using the following representation

$$\delta(x - u_1) = \frac{1}{2\pi} \int_{-\infty}^{+\infty} e^{ik_1(x-u_1)} dk_1 \quad (3.24)$$

and the same for the  $\delta(y - u_2)$ . Starting from the definition (3.1) in accordance with (3.17) and (2.3) one can obtain

$$\begin{aligned} f(x, y) &= \frac{1}{(2\pi)^2} \int_{-\infty}^{+\infty} dk_1 \int_{-\infty}^{+\infty} dk_2 e^{ik_1 x} e^{ik_2 y} \langle e^{-2ik_1 \frac{\hbar}{2m\omega_1} \alpha_1} e^{-2ik_2 \frac{\hbar}{2m\omega_2} \alpha_2} \rangle_{el} \\ &\quad \langle e^{-ik_1 \frac{\hbar}{2m\omega_1} (\tilde{b}_1 + \tilde{b}_1^+)} \rangle_{\tilde{b}_1} \langle e^{-ik_2 \frac{\hbar}{2m\omega_2} (\tilde{b}_2 + \tilde{b}_2^+)} \rangle_{\tilde{b}_2} \end{aligned} \quad (3.25)$$

(due to the variable separation the averaging over the electron and phonon variables is performed independently).

Let us express  $\alpha_r$  operators in terms of the X-operators using the relations (3.21); the following identity is used

$$e^a X^{pp} = (1 - X^{pp}) + e^a X^{pp}. \quad (3.26)$$

As a result, averaged over the electron degrees of freedom part of (3.25) is rewritten in the following form:

$$e^{-ik_1 \zeta_1 (n_1 + n_3 - 2n_2)} e^{-ik_2 \zeta_2 (n_3 - n_1)} = \sum_p e^{-i\vec{k}\vec{\zeta}^{(p)}} X^{pp}, \quad (3.27)$$

where  $\vec{k} = (k_1, k_2)$ ;  $\vec{\zeta}^{(p)} = (\zeta_x^{(p)}; \zeta_y^{(p)})$

$$\begin{aligned} \vec{\zeta}^{(1)} &= (0, 0); & \vec{\zeta}^{(5)} &= (-\zeta_1, -\zeta_2); \\ \vec{\zeta}^{(2)} &= (\zeta_1, -\zeta_2); & \vec{\zeta}^{(6)} &= (2\zeta_1, 0); \\ \vec{\zeta}^{(3)} &= (-2\zeta_1, 0); & \vec{\zeta}^{(7)} &= (-\zeta_1, \zeta_2); \\ \vec{\zeta}^{(4)} &= (\zeta_1, \zeta_2); & \vec{\zeta}^{(8)} &= (0, 0). \end{aligned} \quad (3.28)$$

The following notation is used here:

$$\zeta_r = \frac{\Lambda_r}{m\omega_r^2}. \quad (3.29)$$

After performing the averaging procedure  $X^{pp}$  operators are replaced by their average values:

$$\langle X^{pp} \rangle = e^{-\beta(\lambda_p - \mu N_p)} \left[ \sum_q e^{-\beta(\lambda_q - \mu N_q)} \right]^{-1}. \quad (3.30)$$

In this expression  $N_p$  is the eigenvalue of the electron number operator  $\hat{N} = \sum_p N_p X^{pp}$ . ( $N_1 = 0$ ;  $N_2 = N_3 = N_4 = 1$ ;  $N_5 = N_6 = N_7 = 2$ ;  $N_8 = 3$ )

Average values of exponents including phonon operators in harmonical approximation read:

$$\langle e^{-ik_r \frac{\hbar}{2m\omega_r} (\tilde{b}_r + \tilde{b}_r^+)} \rangle_{\tilde{b}_1} = e^{-\frac{k_r^2}{4m} \frac{\hbar}{\omega_r} (2\tilde{n}_r + 1)}, \quad (3.31)$$

where

$$\tilde{n}_r = \langle \tilde{b}_r^+ \tilde{b}_r \rangle = (e^{\beta \hbar \omega_r} - 1)^{-1}. \quad (3.32)$$

Substituting expressions (3.27) and (3.31) into (3.25) after the integration over the  $k_r$  one can obtain

$$f(x, y) = \frac{1}{4\pi\sqrt{\gamma_1\gamma_2}} \sum_p e^{-\frac{(x-\zeta_x^{(p)})^2}{4\gamma_1}} e^{-\frac{(y-\zeta_y^{(p)})^2}{4\gamma_2}} \langle X^{pp} \rangle. \quad (3.33)$$

This function has a form of the sum of Gauss distributions, centered at the points  $(\zeta_x^{(p)}, \zeta_y^{(p)})$ . Their dispersions are characterized by the parameters

$$\gamma_r = \frac{\hbar}{2m\omega_r} \coth \frac{\beta\hbar\omega_r}{2} \tag{3.34}$$

and statistical weights are determined by the occupation of the corresponding electron states. Schematically it is illustrated in Fig.4 States  $|1\rangle, |3\rangle, |6\rangle, |8\rangle$  correspond to the distributions centered at the origin of the  $y$  variable (e.g.  $u_{ir}$ ). The pairs of states  $|2\rangle, |4\rangle$  and  $|5\rangle, |7\rangle$  correspond to the distributions with double maxima. This means the particle B displacement to the one or another side from the central position (see Fig.5).

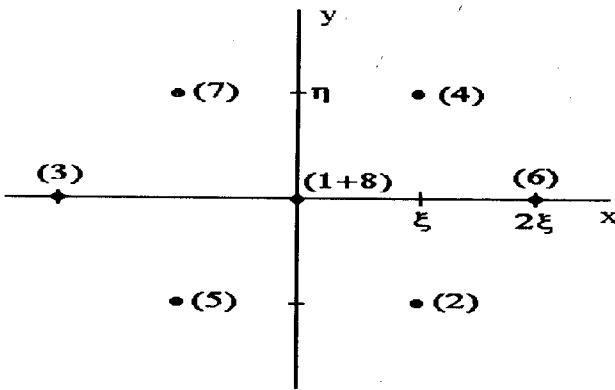


Figure 4. Localization points of Gaussian peaks of function  $f(x, y; \mu)$  ( $\zeta = \frac{\Lambda_r}{m\omega_r^2}$ ;  $\eta = \frac{\Lambda_{ir}}{m\omega_{ir}^2}$ ).

The realization of certain variant depends on the number of electrons in system (if value of  $N$  is fixed) or on the chemical potential value. It depends also on the relations between parameters of the theory.

The equation which connects  $\mu$  and  $N$  and allows to exclude one of these quantities according to (A.26) and (A.29) has the following form

$$\langle \hat{N} \rangle_{x,y} \equiv \frac{\langle \delta(x - u_1)\delta(y - u_2)\hat{N} \rangle}{f(x, y)} = N. \tag{3.35}$$

To get the explicit form of this relation we can exploit the procedure, similar to the one used for obtaining of function  $f(x, y)$ . Mean value  $\langle \delta(x - u_1)\delta(y - u_2)\hat{N} \rangle$  can be presented in the form of integral similar to (3.25). Averaged over the electron variables multiplier in the integrand is equal to

$$\langle e^{-2ik_1 \frac{\hbar}{2m\omega_1} \alpha_1} e^{-2ik_2 \frac{\hbar}{2m\omega_2} \alpha_2} \hat{N} \rangle_{el} = \sum_p e^{i\vec{k}\zeta^{(p)}} N_p \langle X^{pp} \rangle. \tag{3.36}$$

Finally, performing the integration over the variable  $\vec{k}$  we can obtain

$$\langle \delta(x - u_1)\delta(y - u_2)\hat{N} \rangle =$$

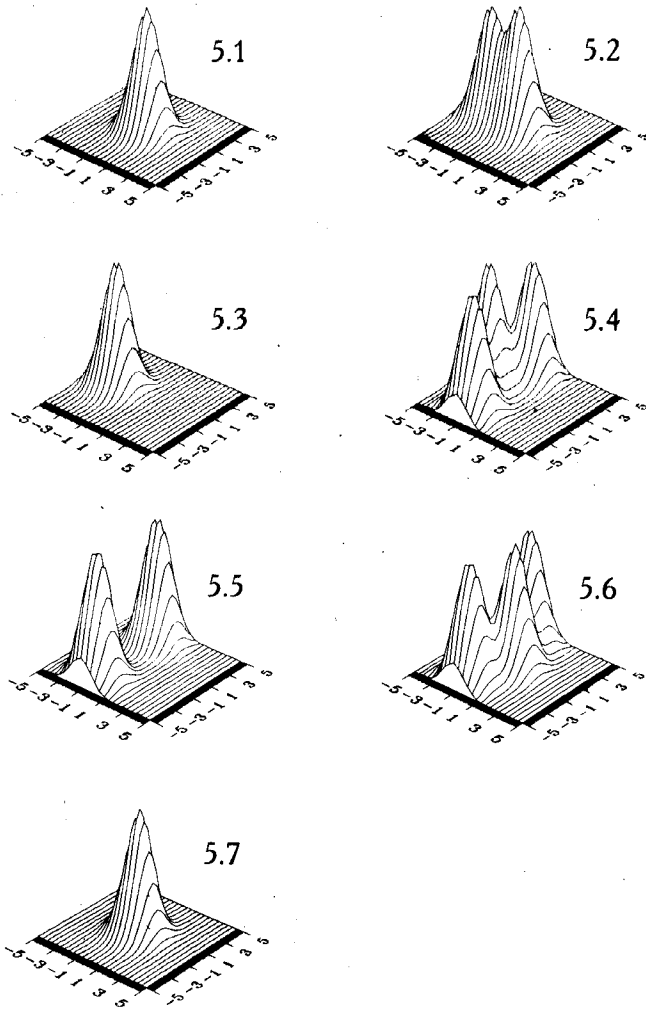


Figure 5. Distribution function  $f(x, y; \mu)$  at different values of chemical potential  $\mu$  (values of chemical potential are given in eV).

5.1  $\mu = -1.00$  ( the corresponding system state is  $|1\rangle$ ).

5.2  $\mu = -0.77$  ( $|1\rangle, |3\rangle$ )

5.3  $\mu = 0.0$  ( $|3\rangle$ )

5.4  $\mu = 0.38$  ( $|3\rangle, |5\rangle, |7\rangle$ )

5.5  $\mu = 0.5$  ( $|5\rangle, |7\rangle$ )

5.6  $\mu = 0.89$  ( $|5\rangle, |7\rangle, |8\rangle$ )

5.7  $\mu = 1.0$  ( $|8\rangle$ )

$$= \frac{1}{4\pi\sqrt{\gamma_1\gamma_2}} \sum_p e^{-\frac{(x-\zeta_x^{(p)})^2}{4\gamma_1}} e^{-\frac{(y-\zeta_y^{(p)})^2}{4\gamma_2}} N_p \langle X^{pp} \rangle \quad (3.37)$$

Subsequently, equation (3.35) can be presented in the form

$$\sum_p e^{-\frac{(x-\zeta_x^{(p)})^2}{4\gamma_1}} e^{-\frac{(y-\zeta_y^{(p)})^2}{4\gamma_2}} (N_p - N) \langle X^{pp} \rangle = 0, \quad (3.38)$$

where mean values  $\langle X^{pp} \rangle$  are given by formula (3.30).

For each Hubbard state  $|p\rangle$  the condition of its realization at  $T \rightarrow 0$  is the minimum condition of the energy of this state. Using this fact, one can analyze possible situations depending on the relations between energy parameters. Obtained results are given in the Fig.6 in the form of  $(\epsilon_1, \epsilon_2)$ - "phase diagrams". Lines on the diagrams separate regions with different types of profiles of function  $f(x, y)$ . When model parameters values correspond to the points lying near such borders, different types of diagrams can coexist. For example, near the border between (2,4) and (3) or (5,7) and (6) phases function  $f(x, y)$  possesses central maximum  $(\zeta_{xI}^{(p)}, 0)$  as well as two symmetrically shifted maxima  $(\zeta_{xII}^{(p)}, \pm\zeta_{yII}^{(p)})$ . It should be noted that (I) and (II) configurations distinguish one from the other not only in displacement of central ion in the second case but also in the change of the cluster length.

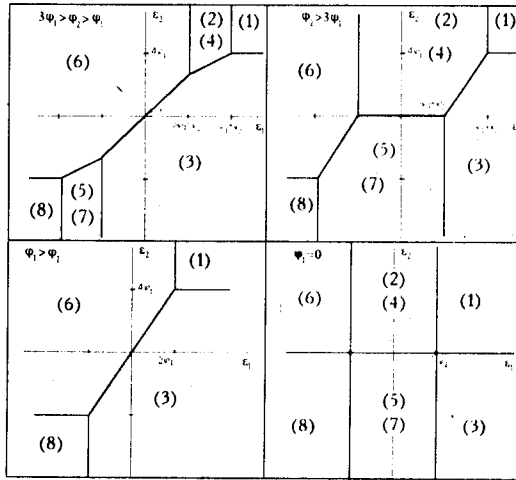


Figure 6.  $(\epsilon_1, \epsilon_2)$ - "phase" diagrams (at zero transfer).

It is important to note that the states with different values of  $\mu$  (with other parameters being the same) are represented on the  $(\epsilon_1, \epsilon_2)$ -diagram by points lying on the straight line  $\epsilon_2 = \epsilon_1 + \delta$ . The position of this line depends on the distance between energy levels of the electrons, localized on the A and B atoms and point location is determined by the relation  $(\epsilon_2 + \epsilon_1)/2 = const - \mu$ . Taking this into account we can determine possible complex configurations as well as the number of electrons at the different values of chemical potential  $\mu$ . Type of the "phase diagram" that is realized in some particular cases depends on the values of electron-phonon interaction constants and on the relations between them.

### 3.3. The role of the electron-electron interactions and spin degrees of freedom

Obtained in item 3.2 results can be generalized by taking into account the Coulomb interactions and Hubbard correlations between electrons and by including spin degeneracy of the orbital states as well as by going beyond the Holstein approximation while describing the electron-phonon interaction (formulae (2.5) and (2.10)). As in previous case, at zero transfer ( $t = 0$ ) the unitary transformation (3.13),(3.14) allows us to separate variables in the similar way; in this case

$$\begin{aligned} \hat{\alpha}_1 &= -\frac{1}{\hbar\omega_1} \sqrt{\frac{\hbar}{2m\omega_1}} \frac{1}{\sqrt{2}} \bar{\gamma}(n_1 + n_3) - \sqrt{2}\gamma'n_2 + \\ &\quad + \frac{1}{\sqrt{2}} \bar{\alpha}n_2(n_1 + n_3) - \sqrt{2}\bar{\beta}n_1n_3 \Big] \\ \hat{\alpha}_2 &= -\frac{1}{\hbar\omega_2} \sqrt{\frac{\hbar}{2m\omega_2}} [\gamma(n_1 - n_3) + \bar{\alpha}n_2(n_1 - n_3)] \sqrt{\frac{M}{2m'}}, \end{aligned} \quad (3.39)$$

where  $\bar{\gamma} = \gamma + 2\beta$ .

After transformation the Hamiltonian can be written in the following form

$$\begin{aligned} \hat{H} &= \sum_i \epsilon_i n_i + U(n_1 + n_3)n_2 + U'n_1n_3 + A(n_{1\uparrow}n_{1\downarrow} + n_{3\uparrow}n_{3\downarrow}) + \\ &\quad + A'n_{2\uparrow}n_{2\downarrow} + \sum_{k=1}^2 \hbar\omega_k \bar{b}_k^+ \bar{b}_k - \sum_{k=1}^2 \hbar\omega_k \hat{\alpha}_k^2, \end{aligned} \quad (3.40)$$

or, on the basis of states  $|n_{1\uparrow}n_{1\downarrow}n_{2\uparrow}n_{2\downarrow}n_{3\uparrow}n_{3\downarrow}\rangle$ ,

$$\hat{H} = \sum_q \lambda_q X^{qq} + \sum_k \hbar\omega_k \bar{b}_k^+ \bar{b}_k \quad (3.41)$$

(the notations are given in Appendix 2)

Evaluation of the distribution function  $f(x, y)$  can be performed similarly to the previous case (see 3.2). Expressing operators  $\hat{\alpha}_k$  in terms of the  $X$ -operators

$$\hat{\alpha}_k = -\frac{1}{\hbar\omega_k} \sqrt{\frac{\hbar}{2m\omega_k}} \sum_q A_q^{(k)} X^{qq} \quad (3.42)$$

and using the following representation

$$e^{-2ik_i \sqrt{\frac{\hbar}{2m\omega_i}} \hat{\alpha}_i} = \sum_q e^{ik_i \frac{1}{m\omega_i^2} A_q^{(i)}} X^{qq} \quad (3.43)$$

we obtain

$$\langle e^{-2i \sum_i k_i \sqrt{\frac{\hbar}{2m\omega_i}} \hat{\alpha}_i} \rangle = \sum_q e^{-i \sum_i \frac{k_i}{m\omega_i^2} A_q^{(i)}} \langle X^{qq} \rangle. \quad (3.44)$$

As a result, using (3.25) and (3.31) we have.



$$f(x, y) = \frac{1}{4\pi\sqrt{\gamma_1\gamma_2}} \sum_q \langle X^{qq} \rangle \exp \left\{ -\frac{(x - \frac{A_q^{(1)}}{m\omega_1^2})^2}{4\gamma_1} \right\} \exp \left\{ -\frac{(y - \frac{A_q^{(2)}}{m\omega_2^2})^2}{4\gamma_2} \right\}. \quad (3.45)$$

The last expression has a structure similar to (3.33). Coordinates of the points corresponding to the Gaussian components maxima are determined now by the coefficients  $A_q^{(i)}$  (their explicit expressions are given in the Appendix 3). There are much more components than in the previous case when we considered only Holstein type interactions. That is why  $(\epsilon_1, \epsilon_2)$ -diagrams have more complicated structure and include more possible phases. Even in the spinless case the existence of the Coulomb interactions between electron changes the geometry of the phase diagrams and causes the appearance of their new types (see Fig. 7). Possible forms of  $(\epsilon_1, \epsilon_2)$ -diagrams in the case when spin variables are taken into account are given on Fig.8 for some values of model parameters. Number of electrons on the cluster in various states are also given there. In the states with the energies  $\lambda_2$  (one electron),  $\lambda_8, \lambda_9$  (two electrons),  $\lambda_{23}, \lambda_{25}, \lambda_{27}$  (three electrons),  $\lambda_{43}, \lambda_{44}$  (four electrons),  $\lambda_{58}$  (five electrons) effective potential possesses two minima.

Diagrams corresponding to the case which was considered in [7] (the cluster  $O-Cu-O$  in the crystal  $YBa_2Cu_3O_{7-\delta}$ ), are presented on Fig 9,10. The charge state  $O^{2-}-Cu^{1+}-O^{2-}$  of the cluster was taken as the initial one (this corresponds to the values of charges  $z_1 = z_3 = -2, z_2 = +1$ ); the presence of two holes on cluster was considered. The Hamiltonian of the cluster was written in the form (2.4), (2.5) and (2.10) with the excluding of terms describing electron transfer. Operators  $a_{i\sigma}^\dagger, a_{i\sigma}$  were considered to be the creation and annihilation operators of the holes. Correspondingly, the changes were introduced into the electrostatic components of interactions:  $\gamma \rightarrow \gamma_0 + \frac{e^2}{d^2} z_2$ ;  $\gamma' \rightarrow \gamma'_0 - \frac{e^2}{d^2} z_1$ ;  $\beta \rightarrow \frac{e^2}{4d^2} z_1$ ;  $\epsilon_1 \rightarrow \epsilon_1^0 + \frac{e^2}{d} z_2 + \frac{e^2}{2d} z_1$ ,  $\epsilon_2 \rightarrow \epsilon_2^0 + 2\frac{e^2}{d} z_1$ .

Two cases were examined. In the first one as in [7] the simplified Hamiltonian where Coulomb interactions were not included (except Hubbard correlations) was considered. The electron-vibrational interaction was written similar to (3.12), but spin degeneracy was still present ( $n_i = \sum_\sigma n_{i\sigma}$ ). The relations were assumed:

$$\begin{aligned} \frac{1}{\sqrt{2}}(\gamma + 2\beta) &= \frac{1}{\sqrt{2}}\gamma' = -\Lambda_r \\ \sqrt{\frac{M}{2m'}}\gamma &= -\Lambda_{ir} \end{aligned} \quad (3.46)$$

According to the data, presented in the [7,9], the following values of parameters were used:

$$\begin{aligned} \epsilon_1 &= 0.5eV; \quad \hbar\omega_{ir} = 500cm^{-1}; \quad \Delta = -0.13\frac{e^2}{d} \\ \epsilon_2 &= -0.5eV; \quad \hbar\omega_r = 600cm^{-1}; \quad d = 1.85A \end{aligned}$$

Obtained  $(\epsilon_1, \epsilon_2)$ -phase diagrams are presented in the Fig. 9.1-9.4 for the different values of the interactions constants  $\Lambda_{ir}, \Lambda_{i\sigma}$  and  $A$  and  $A'$  parameters. Values of parameters  $\tau_i$ , determining the correlational corrections

	$\begin{cases} \tau_4 > 2\tau_1 \\ \tau_5 - \tau_4 < \tau_2 \\ 2\tau_3 - \tau_2 < \tau_5 \end{cases}$		$\begin{cases} \tau_4 > 2\tau_1 \\ \tau_5 - \tau_4 > \tau_2 \\ 2\tau_3 - \tau_2 < \tau_5 \end{cases}$
	$\begin{cases} \tau_4 < 2\tau_1 \\ \tau_5 - 2\tau_4 < \tau_2 - 2\tau_1 \\ 2\tau_3 - \tau_2 < \tau_5 \end{cases}$		$\begin{cases} \tau_4 < 2\tau_1 \\ 2\tau_1 + \tau_2 < \tau_5 \\ 2\tau_3 - \tau_2 < \tau_5 \end{cases}$
	$\begin{cases} \tau_4 < 2\tau_1 \\ 2\tau_3 - 2\tau_2 < \tau_4 \\ 2\tau_3 - \tau_2 > \tau_5 \end{cases}$		$\begin{cases} \tau_4 < 2\tau_1 \\ 2\tau_3 + \tau_4 < 2\tau_5 \\ 2\tau_3 - \tau_2 < \tau_5 \end{cases}$
	$\begin{cases} \tau_4 < 2\tau_1 \\ 2\tau_3 - \tau_2 > \tau_5 \\ 2\tau_3 - \tau_2 > \tau_5 \end{cases}$		$\begin{cases} \tau_4 < 2\tau_1 \\ \tau_1 + \tau_3 < \tau_5 \\ 2\tau_3 - \tau_2 > \tau_5 \end{cases}$
	$\begin{cases} \tau_4 < 2\tau_1 \\ 2\tau_3 - 2\tau_2 > \tau_4 \\ 2\tau_3 + \tau_4 > 2\tau_5 \end{cases}$		$\begin{cases} 2\tau_1 + \tau_2 > \tau_5 \\ 2\tau_3 - \tau_2 < \tau_5 \\ \tau_5 - 2\tau_4 > \tau_2 - 2\tau_1 \end{cases}$
	$\begin{cases} \tau_1 - \tau_3 < \tau_4 - \tau_5 \\ 2\tau_3 - 2\tau_2 < \tau_4 \\ \tau_2 - \tau_1 < \tau_3 - \tau_4 \end{cases}$		$\begin{cases} \tau_1 - \tau_3 > \tau_4 - \tau_5 \\ \tau_1 + \tau_2 - \tau_3 < 0 \\ \tau_1 + \tau_3 - \tau_5 > 0 \end{cases}$
	$\begin{cases} \tau_1 - \tau_3 < \tau_4 - \tau_5 \\ \tau_1 + \tau_2 - \tau_3 < 0 \\ \tau_2 - \tau_1 < \tau_3 - \tau_4 \end{cases}$		$\begin{cases} \tau_1 - \tau_3 > \tau_4 - \tau_5 \\ 2\tau_3 - \tau_2 > \tau_5 \\ \tau_1 + \tau_2 - 3 > 0 \end{cases}$

Figure 7. The types of  $(\epsilon_1, \epsilon_2)$ -“phase” diagrams in the spinless case taking into account the Coulomb interactions.  $\tau_p = \lambda_p - \sum_i \epsilon_i n_i$ .

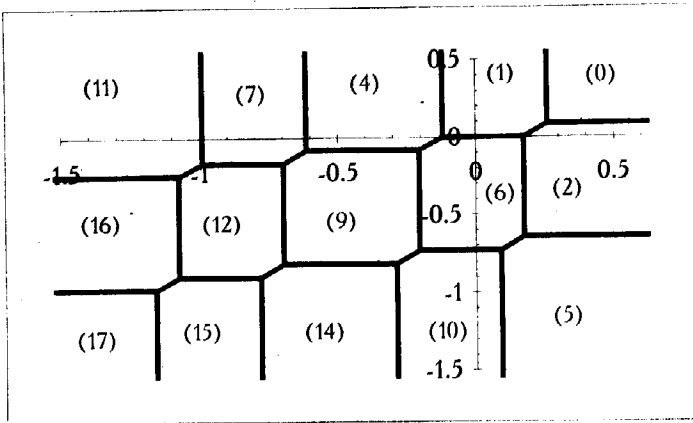


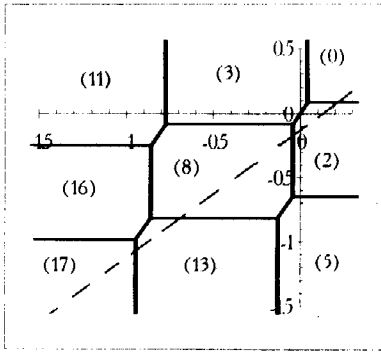
Figure 8.  $(\epsilon_1, \epsilon_2)$ -phase diagrams of the complex taking into account the spin variables.

$\tau_1 = 0.26$	$\tau_5 = -0.56$	$\tau_9 = 0.06$	$\tau_{13} = -0.82$	$\tau_{17} = -2.70$
$\tau_2 = 0.08$	$\tau_6 = 0.26$	$\tau_{10} = -0.47$	$\tau_{14} = -0.76$	
$\tau_3 = 0.08$	$\tau_7 = -0.47$	$\tau_{11} = -1.46$	$\tau_{15} = -1.54$	
$\tau_4 = 0.14$	$\tau_8 = 0$	$\tau_{12} = -0.64$	$\tau_{16} = -1.71$	

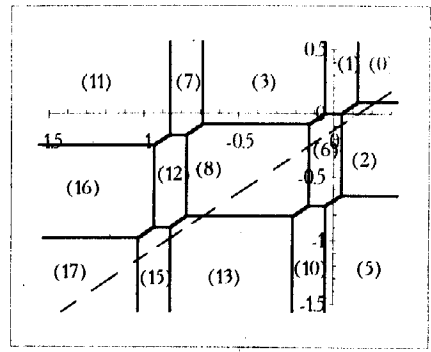
Phase (0) corresponds to the  $N = 0$  electrons in cluster; (1),(2) -  $N = 1$ ; (3),(4),(5),(6) -  $N = 2$ ; (7),(8),(9),(10) -  $N = 3$ ; (11),(12),(13),(14) -  $N = 4$ ; (15),(16) -  $N = 5$ ; (17) -  $N = 6$ .

to the energies of the electron states ( $\tau_p = \lambda_p - \sum_{i\sigma} \epsilon_i n_{i\sigma}^{(p)}$ ) are also given there. Trajectories describing the change of the state of the system at the change of chemical potential  $\mu$  (or , correspondingly, the change of mean number of holes  $N$ ), are depicted on figures. At  $N = 2$  the point representing the state of system belongs to the region of the states with energies  $\lambda_9$ . Corresponding effective potential possesses two minima in this case; distribution function  $f(x, y)$  has two Gaussian components centered at the points  $(\frac{A_q^{(1)}}{m\omega_1^2}; \pm \frac{A_q^{(2)}}{m\omega_2^2})$  (charge state of the complex is  $O^{1-} - Cu^{2+} - O^{1-}$  or  $O^{2-} - Cu^{2+} - O^{1-}$ ). Such property takes place when parameter  $\Lambda_{ir}$  exceeds some critical value and is realized in rather wide range of constants  $A$  and  $A'$  values (however, it disappears at  $A, A' \rightarrow 0$ ). These results are in accordance with those of [7].

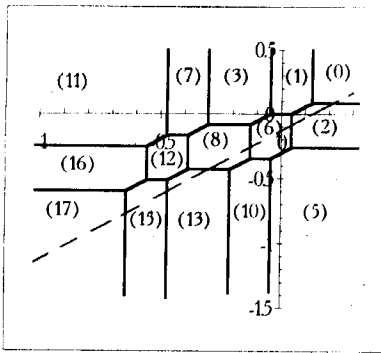
In the second considered case we start from the more general Hamiltonian (2.10). The account of the electrostatic interaction shifts the trajectory determining the change of the state of system to the positive direction of the ordinate axis. It also changes significantly the values of correlation corrections  $\tau_i$ . Phase diagrams in this case are shown at Fig. 10.1-10.4 for the different values of  $A$  and  $A'$  parameters. In the first case ( $A = A' = 7\text{eV}$ ) at  $N = 2$  only the phase with the energy  $\lambda$  is realized. Electron distribution is symmetrical (charge state  $O^{1-} - Cu^{1+} - O^{1-}$ ), effective potential possesses only central minimum. At the decrease of the correlation energy  $A$  on the oxygen atom the ground state is changed  $\lambda_{11} \rightarrow \lambda_8$  (Fig.10.2). State with energy  $\lambda_8$  (two holes on the one of the oxygen atoms:  $O^0 - Cu^{1+} - O^{2-}$  or  $O^{2-} - Cu^{1+} - O^0$ ) is characterized by the effective potential with double



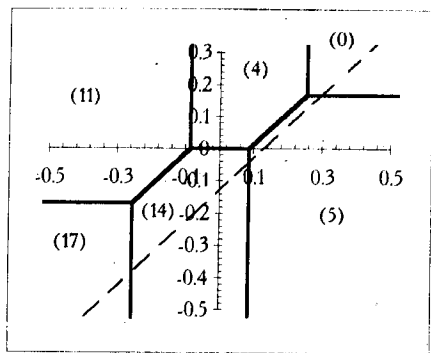
9.1



9.2



9.3



9.4

Figure 9.  $(\epsilon_1, \epsilon_2)$ -phase diagrams for the cluster O-Cu-O in YBaCuO crystal (calculated on the basis of the simplified model [7]).  $\epsilon_1 = 0.5$  eV;  $\epsilon_2 = -0.5$  eV;  $\Lambda_r = 0.1$ ,  $\hbar\omega_r = 500\text{cm}^{-1}$ ,  $\hbar\omega_{ir} = 600\text{cm}^{-1}$ ,

9.1  $\Lambda_{ir} = 0.1$  eV  $A = A' = 7$  eV

9.2  $\Lambda_{ir} = 0.2$  eV  $A = A' = 7$  eV

9.3  $\Lambda_{ir} = 0.2$  eV  $A = A' = 4$  eV

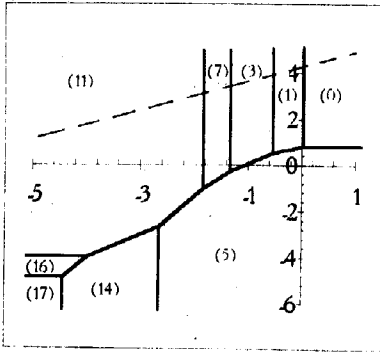
9.4  $\Lambda_{ir} = 0.2$  eV  $A = A' = 0$

symmetrical minimum. When the Coulomb interactions besides the short-range ones are included, the form of  $(\epsilon_1, \epsilon_2)$ -diagrams remains the same at the change of the short range interaction parameters in sufficiently wide range (see Fig. 10.3-10.4).

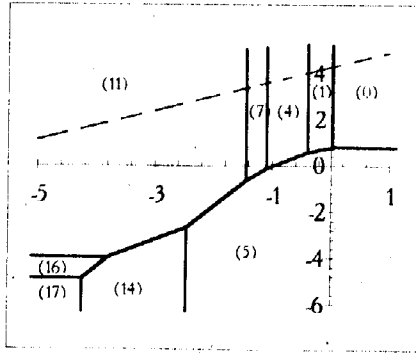
Our results show that Coulomb electron-electron and electron-ion interactions influence to a great extent on the form of  $(\epsilon_1, \epsilon_2)$ -diagrams as well as on the ground state of the complex and its configuration. They change the criteria of appearance of the locally anharmonic potential determining the IR dynamics of the complex.

#### 4. Energy spectrum at the presence of the electron transfer

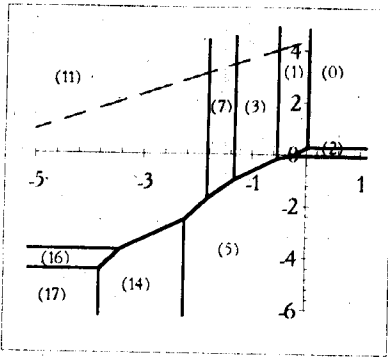
Basing on the obtained above results, we will examine the role of electron transfer in formation of the ground state and in dynamics of the system. We will use simplified model, studied in item 3.1. Energy of the electron



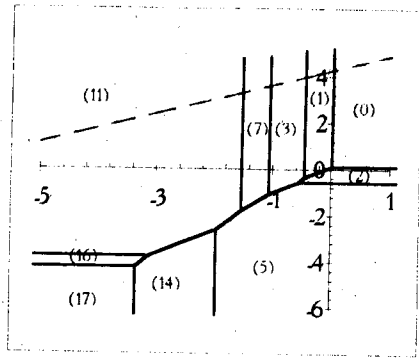
10.1



10.2



10.3



10.4

Figure 10.  $(\epsilon_1, \epsilon_2)$ -phase diagrams for cluster O-Cu-O in YBaCuO crystal taking into account spin degrees of freedom.  $\epsilon_1 = 0.5$  eV;  $\epsilon_2 = -0.5$  eV;  $z_1 = z_3 = +2e$ ,  $z_2 = -1e$ ,  $\hbar\omega_r = 500\text{cm}^{-1}$ ,  $\hbar\omega_{ir} = 600\text{cm}^{-1}$ .

- 10.1  $A = 7$  eV,  $A' = 7$  eV,  $\gamma' = 0$ ,  $\gamma'_0 = 0$
- 10.2  $A = 4$  eV,  $A' = 7$  eV,  $\gamma' = 0$ ,  $\gamma'_0 = 0$
- 10.3  $A = 7$  eV,  $A' = 7$  eV,  $\gamma' = 0$ ,  $\gamma'_0 = -0.67 e^2/d^2$
- 10.4  $A = 7$  eV,  $A' = 7$  eV,  $\gamma' = -0.5 e^2/d^2$ ,  $\gamma'_0 = -1.17 e^2/d^2$

transfer

$$H_{tr} = t(a_1^+ a_2 + a_2^+ a_1 + a_2^+ a_3 + a_3^+ a_2) \tag{4.1}$$

is added to the Hamiltonian of the model, which at the quantum description of vibrations has the form (3.12).

Application of the displacement transformation (3.13) doesn't lead at  $t \neq 0$  to the separation of the electron and phonon variables. Due to

$$\begin{aligned} e^{\hat{S}} a_1 e^{-\hat{S}} &= e^{\xi_2 - \xi_1} a_1; \\ e^{\hat{S}} a_2 e^{-\hat{S}} &= e^{2\xi_1} a_2; \\ e^{\hat{S}} a_3 e^{-\hat{S}} &= e^{-(\xi_1 + \xi_2)} a_3, \end{aligned} \tag{4.2}$$

where

$$\xi_i = \sqrt{\frac{\hbar}{2m\omega_i}} \frac{\Lambda_i}{\hbar\omega_i} (\tilde{b}_i - \tilde{b}_i^+); \xi_i = -\xi_i^+ \tag{4.3}$$

we can see, that

$$e^{\hat{S}} H_{tr} e^{-\hat{S}} = t[a_1^+ a_2 e^{3\xi_1 - \xi_2} + a_2^+ a_1 e^{\xi_2 - 3\xi_1} + a_2^+ a_3 e^{-3\xi_1 - \xi_2} + a_3^+ a_2 e^{3\xi_1 + \xi_2}]. \quad (4.4)$$

Electron transfer between ions is accompanied by the shifts of the ion equilibrium positions; this is expressed by the existence of the exponential displacement operators.

After transition to the Hubbard representation on the basis of states (3.20) the Hamiltonian of the model becomes

$$\begin{aligned} \hat{H} = & \sum_p \lambda_p X^{pp} + \sum_r \hbar \omega_r \tilde{b}_r^+ \tilde{b}_r + \\ & + t \left[ (X^{23} + X^{67}) e^{3\xi_1 - \xi_2} + (X^{32} + X^{76}) e^{\xi_2 - 3\xi_1} + \right. \\ & \left. + (X^{34} + X^{56}) e^{-3\xi_1 - \xi_2} (X^{43} + X^{65}) e^{3\xi_1 + \xi_2} \right]. \end{aligned} \quad (4.5)$$

In the case of strong coupling between electrons and phonons we can use mean field approximation performing the decoupling

$$\begin{aligned} (X^{23} + X^{67}) e^{3\xi_1 - \xi_2} & \rightarrow (X^{23} + X^{67}) \langle e^{3\xi_1 - \xi_2} \rangle + \\ & + \langle X^{23} + X^{67} \rangle e^{3\xi_1 - \xi_2} - \langle X^{23} + X^{67} \rangle \langle e^{3\xi_1 - \xi_2} \rangle. \end{aligned} \quad (4.6)$$

As a result, Hamiltonian is separated into the phonon and electron parts:

$$\hat{H}_{MF} = \hat{H}_{MF}^{ph} + \hat{H}_{MF}^{el} + U; \quad (4.7)$$

$$\begin{aligned} \hat{H}_{MF}^{el} = & \sum_p \lambda_p X^{pp} + \tilde{t} (X^{23} + X^{32} + X^{34} + X^{43} + \\ & + X^{56} + X^{65} + X^{67} + X^{76}), \end{aligned} \quad (4.8)$$

$$\begin{aligned} \hat{H}_{MF}^{ph} = & \sum_r \hbar \omega_r \tilde{b}_r^+ \tilde{b}_r + t \langle X^{23} + X^{67} \rangle (e^{3\xi_1 - \xi_2} + e^{\xi_2 - 3\xi_1}) + \\ & + \langle X^{34} + X^{56} \rangle (e^{-3\xi_1 - \xi_2} + e^{3\xi_1 + \xi_2}), \end{aligned} \quad (4.9)$$

where

$$\tilde{t} = t e^{-g} \equiv t \langle e^{\pm 3\xi_1} \rangle \langle e^{\pm \xi_2} \rangle \quad (4.10)$$

is the renormalized electron transfer integral<sup>3</sup>. The mean values of electron and phonon operators will be determined here self-consistently using the Hamiltonians (4.8) and (4.9). In zeroth approximation

$$\langle e^{\pm 3\xi_1} \rangle = e^{-g_1}; \quad \langle e^{\pm \xi_2} \rangle = e^{-g_2}, \quad (4.11)$$

where

$$g_\alpha = \frac{\Lambda_\alpha^2}{4m\hbar\omega_\alpha^3} \coth \frac{\beta\hbar\omega_\alpha}{2}. \quad (4.12)$$

<sup>3</sup>Effect of band width renormalization is typical to the systems of narrow-band electron coupled to a bosonic field (see, for example, [10])

Factor  $e^{-g}$  leads to the effective decrease of the transfer parameter - such decrease may be significant at the  $\Lambda_\alpha \gg 2\omega_\alpha \sqrt{m\hbar\omega_\alpha}$ .

Electron transfer leads to the splitting of the electron spectrum levels  $\lambda_2 = \lambda_4$ ,  $\lambda_2 = \lambda_4$ .

$$\begin{aligned}\tilde{\lambda}_{2,3} &= \frac{1}{2}(\lambda_2 + \lambda_3) \pm \Pi_1; \\ \tilde{\lambda}_4 &= \lambda_4 \\ \tilde{\lambda}_{5,6} &= \frac{1}{2}(\lambda_5 + \lambda_6) \pm \Pi_2; \\ \tilde{\lambda}_7 &= \lambda_7;\end{aligned}\tag{4.13}$$

$$\Pi_1 = [(\frac{\lambda_2 - \lambda_3}{2})^2 + 2t^2]^{1/2}; \quad \Pi_2 = [(\frac{\lambda_5 - \lambda_6}{2})^2 + 2t^2]^{1/2}.\tag{4.14}$$

In the case when level  $\lambda_2 = \lambda_4$  ( $N = 1$ ) determines the ground state of the system (at  $t = 0$ ) a doublet caused by the influence of electron transfer appears at  $e^{-g} \ll t$  with distance between sublevels

$$\Delta = \frac{2t^2}{\lambda_3 - \lambda_2}.\tag{4.15}$$

The same picture can be observed at  $N = 2$  when instead of level  $\lambda_5 = \lambda_7$  doublet with the distance between sublevels

$$\Delta' = \frac{2t^2}{\lambda_6 - \lambda_5}\tag{4.16}$$

appears.

Due to the different parity of the wave functions of sublevels

$$\begin{aligned}|\tilde{2}\rangle &= \frac{1}{\sqrt{2}}(|2\rangle + |4\rangle) \cos \theta_1 + |3\rangle \sin \theta_1; \\ |\tilde{3}\rangle &= -\frac{1}{\sqrt{2}}(|2\rangle + |4\rangle) \sin \theta_1 + |3\rangle \cos \theta_1; \\ |\tilde{4}\rangle &= -\frac{1}{\sqrt{2}}(|4\rangle - |2\rangle); \end{aligned}\tag{4.17}$$

$$\sin \theta_1 = \frac{\sqrt{2}t}{\lambda_2 - \lambda_3};\tag{4.18}$$

the dipole transitions  $|\tilde{2}\rangle \leftrightarrow |\tilde{4}\rangle \leftrightarrow |\tilde{3}\rangle$  are allowed. First of them corresponds to the energy  $\Delta$  and in the considered case can belong to the IR-frequency range of spectrum. Energy splitting (4.15) or (4.16) between symmetrical and antisymmetrical states is analogous to the splitting between two lowest energy levels of the particle in the double-well potential. However, in the present case the coupled motion takes place: the ion displacements are accompanied by the electron redistribution. The appearance of the doublets with transition energies  $\Delta$  and  $\Delta'$  is the result of the quipolaron effect (see also [9]).

At large enough distances between the doublet and the next excited levels pseudospin formalism (with effective spin  $S = 1/2$ ) can be applied to the

description of the dipole transitions in the complex and interactions between complexes. This fact justifies the possibility of the applying the pseudospin model to the description of sublattice in crystal with local anharmonicity in the case when this anharmonicity is caused by the electron-phonon interaction. Such model is used in the description of dynamics of apex oxygen ions in the high temperature superconducting systems of YBaCuO-type [17-19].

## 5. Conclusions

The problem concerning adiabatic potentials, ion distribution functions and equilibrium complex configurations was investigated on the example of the ion cluster A-B-A taken as an element of the one-dimensional structure. The energy spectrum of the model was studied; the conditions of the formation of locally anharmonic lattice vibrations are analyzed.

The Hamiltonian written in the strong coupling approximation for electron subsystem was used for the model description. The interaction with the ion vibrations along the axis of the complex was considered; two harmonical phonon modes ( $u_r, u_{ir}$ ) which are infrared- and Raman-active correspond to them. The shift of the energy levels of the electrons localized at the particular ions and change of the transfer integral values caused by the mutual displacements were also taken into account.

The expression for the free energy functional  $F(u_r, u_{ir})$ , which can be treated as the effective adiabatic potential was obtained on the basis of the proposed model with the help of the averaging procedure over the states of electron subsystem. The behaviour of the function  $F(u_r, u_{ir})$  as well as the ion distribution function  $\rho(u_r, u_{ir}) = \exp[\beta(F(u_r, u_{ir}) - F_0)]$  as functions of the model parameters (distance between energy levels  $\epsilon_A, \epsilon_B$ , the coupling constants, the mean value of electron number on the complex) was investigated.

It was shown that the effective potential can possess one  $(x, y) = (0, U_r)$  or two  $(x, y) = (\pm U_{ir}, U_r)$  symmetrical minima; in some cases they can coexist. At the absence of the electron transfer the distribution function  $f(x, y)$  is of Gaussian type in the vicinity of these points and ion vibrations remain harmonical due to the variable separation. The dependence of ion distribution functions and effective potentials on temperature, coupling constants, relative positions of electron energy levels and charge state of A-B-A' complex were investigated in the regimes  $\mu = \text{const}$  and  $n = \text{const}$ . The phase diagrams separating the areas of parameter values with different topological types of effective anharmonic potentials were plotted.

It was shown that in the case of double-minima potential the doublet is formed in the low-lying part of spectrum; this doublet can be treated as the splitted by tunneling pair of levels (with sublevel distance of the order of  $t \cdot e^{-g}$ ). This is caused by quasipolaronic effect connected with process of simultaneous ion displacements and redistribution of electron density in the system. Numerical calculations were performed with the use of parameter values corresponding to the complexes O-Cu-O in the high- $T_c$  superconducting crystals of YBaCuO type.

## Appendix 1. Distribution functions and "conditional" thermodynamic functions.

Distribution function, characterizing for the thermodynamically equilibrium system the probabilities of the certain values of the physical variable



described by the operator  $\hat{A}$  can be introduced according to the definition

$$f(a) = \langle \delta(a - \hat{A}) \rangle, \quad (\text{A.1})$$

where  $\langle \dots \rangle$  is statistical averaging over the canonical Gibbs ensemble. Function (A.1) satisfies the following normalization condition

$$\int f(a) da = 1. \quad (\text{A.2})$$

a) In the case of the system described by the canonical distribution

$$f(a) = \frac{Z(a)}{Z};$$

$$Z(a) = Sp[\delta(a - \hat{A})e^{-\beta\hat{H}}]; \quad Z = Sp e^{-\beta\hat{H}}. \quad (\text{A.3})$$

Beside the usual statistical operator

$$\hat{\rho}_0 = \frac{1}{Z} e^{-\beta\hat{H}} \quad (\text{A.4})$$

we will use so-called extended statistical operator

$$\hat{\rho}(a) = \delta(a - \hat{A})\hat{\rho}_0, \quad (\text{A.5})$$

$\hat{\rho}_0$  can be obtained from (A.5) by integration over variable  $a$

$$\hat{\rho}_0 = \int \hat{\rho}(a) da \quad (\text{A.6})$$

and function  $f(a)$  can be obtained by performing the trace operation

$$f(a) = Sp \hat{\rho}(a). \quad (\text{A.7})$$

The ratio

$$\frac{\hat{\rho}(a)}{f(a)} \equiv \hat{\rho}|_a \quad (\text{A.8})$$

has the meaning of conditional probability density;  $\hat{\rho}|_a$  can be called "conditional" statistical operator. The following normalization condition must be satisfied:

$$Sp \hat{\rho}|_a = 1. \quad (\text{A.9})$$

We can introduce conditional mean values similarly to the common thermodynamical averages  $\langle B \rangle = Sp(\hat{B}\hat{\rho}_0)$  in the following way:

$$\langle B \rangle|_a = Sp(\hat{B}\hat{\rho}|_a) = \frac{Sp(\hat{B}\hat{\rho}(a))}{f(a)}. \quad (\text{A.10})$$

In the last expression the numerator

$$Sp(\hat{B}\hat{\rho}(a)) = Sp(\hat{B}\delta(a - \hat{A})\hat{\rho}_0) = \langle B \rangle|_a f(a) \equiv B(a) \quad (\text{A.11})$$

plays the role of density for the  $\langle B \rangle$ :

$$\int B(a) da = Sp(\hat{B}\hat{\rho}_0) = \langle B \rangle. \quad (\text{A.12})$$

In particular, according to this definition we can introduce "conditional" internal energy:

$$\langle H \rangle|_a \equiv U|_a = \frac{Sp(\hat{H}\hat{\rho}(a))}{f(a)} = \frac{H(a)}{f(a)}. \quad (\text{A.13})$$

"Conditional" free energy can be obtained from the  $Z(a)$  by means of the following relation:

$$Z(a) = e^{-\frac{F|_a}{\theta}}. \quad (\text{A.14})$$

In this case <sup>4</sup>

$$f(a) = \frac{1}{Z} e^{-\frac{F|_a}{\theta}} = e^{\frac{F-F|_a}{\theta}} \quad (\text{A.15})$$

and

$$F|_a = -\theta \ln Z(a) = -\theta \ln Sp[\delta(a - \hat{A})e^{-\beta\hat{H}}]. \quad (\text{A.16})$$

It results, as one can see, in the following

$$-\frac{\partial F|_a}{\partial \theta} = \ln Z(a) + \frac{1}{\theta} \frac{H(a)}{Z(a)} Z = -\frac{F|_a - U|_a}{\theta}, \quad (\text{A.17})$$

this corresponds to the usual thermodynamical relation between free and internal energies. Using the (A.17) we can introduce function

$$S|_a = -\frac{\partial F|_a}{\partial \theta}, \quad (\text{A.18})$$

which can be interpreted as "conditional" entropy.

b) Relations given in item a) can be easily transferred to the case with variable number of particles that can be described using the grand canonical ensemble. Distribution function over the variable  $a$  now can be written

$$\begin{aligned} f(a; \mu) &= \frac{1}{Z} Sp[\delta(a - \hat{A})e^{-\beta(\hat{H} - \mu\hat{N})}], \\ Z &= Sp e^{-\beta(\hat{H} - \mu\hat{N})}. \end{aligned} \quad (\text{A.19})$$

Using the following definition

$$Z(a; \mu) = Sp[\delta(a - \hat{A})e^{-\beta(\hat{H} - \mu\hat{N})}], \quad (\text{A.20})$$

we can write:

$$f(a, \mu) = \frac{1}{Z} Z(a; \mu). \quad (\text{A.21})$$

<sup>4</sup>Expression (A.15) is an analogy of the expression for the probability of fluctuations (deviations from the average value) of the physical quantities. The proposed scheme of introducing the conditional thermodynamic functions is similar to the one used in [20].

The "conditional" thermodynamical potential can be introduced similarly to the free energy:

$$\Phi|_a = -\theta \ln Z(a; \mu). \quad (\text{A.22})$$

One can ensure that

$$-\frac{\partial \Phi|_a}{\partial \theta} = -\frac{\Phi|_a}{\theta} + \frac{\langle \hat{H} - \mu \hat{N} \rangle|_a}{\theta} = \frac{U|_a - F|_a}{\theta} = S|_a, \quad (\text{A.23})$$

because

$$F|_a = \Phi|_a + \mu \langle \hat{N} \rangle|_a, \quad (\text{A.24})$$

as well as

$$-\frac{\partial \Phi|_a}{\partial \mu} = \frac{Sp[\delta(a - \hat{A}) \hat{N} e^{-\beta(\hat{H} - \mu \hat{N})}]}{f(a; \mu) Z} = \langle \hat{N} \rangle|_a. \quad (\text{A.25})$$

The last expression at given mean number of particles

$$\langle \hat{N} \rangle|_a = N \quad (\text{A.26})$$

defines the value of the chemical potential as the function of the variable  $a$ . From the other point of view, when external conditions ( thermostat) fix the constant value of  $\mu$ , then in accordance with (A.25) number of particles is the function of  $a$ .

Similarly to (A.14) function  $f(a; \mu)$  can be represented in the following form:

$$f(a, \mu) = \exp\left(\frac{\Phi - \Phi|_a}{\theta}\right). \quad (\text{A.27})$$

Using the condition (A.26) and expression (A.24) at the fixed value of average particles number this distribution can be rewritten similarly to (A.15). The most probable values of  $a$  correspond to the functions  $f(a)$  or  $f(a; \mu)$  maxima, or, what is the same, to the  $F|_a$  or  $\Phi|_a$  minima; these minima define the equilibrium states of the system at the given  $N$  or  $\mu$  values respectively.

It can be mentioned that for the grand canonical ensemble "conditional" statistical operator has the following form

$$\hat{\rho}|_{a; \mu} = \frac{\delta(a - \hat{A}) \frac{1}{Z} e^{-\beta(\hat{H} - \mu \hat{N})}}{f(a; \mu)} \quad (\text{A.28})$$

and the conditional average of the  $\hat{B}$  operator is equal to

$$\langle B \rangle|_{a; \mu} = Sp(\hat{B} \hat{\rho}|_{a; \mu}). \quad (\text{A.29})$$

**Appendix 2. Basis functions  $|n_1 \uparrow n_1 \downarrow n_2 \uparrow n_2 \downarrow n_3 \uparrow n_3 \downarrow$  and corresponding values of energy.**

	$p >$	$\lambda_p$		$p >$	$\lambda_p$
000000 >	1 >	$\lambda_1$	011100 >	33 >	$\lambda_{27}$
100000 >	2 >	$\lambda_2$	011010 >	34 >	$\lambda_{28}$
010000 >	3 >	$\lambda_2$	011001 >	35 >	$\lambda_{28}$
001000 >	4 >	$\lambda_4$	010110 >	36 >	$\lambda_{28}$
000100 >	5 >	$\lambda_4$	010101 >	37 >	$\lambda_{28}$
000010 >	6 >	$\lambda_2$	010011 >	38 >	$\lambda_{25}$
000001 >	7 >	$\lambda_2$	001110 >	39 >	$\lambda_{27}$
110000 >	8 >	$\lambda_8$	001101 >	40 >	$\lambda_{27}$
101000 >	9 >	$\lambda_9$	001011 >	41 >	$\lambda_{23}$
100100 >	10 >	$\lambda_9$	000111 >	42 >	$\lambda_{23}$
100010 >	11 >	$\lambda_{11}$	111100 >	43 >	$\lambda_{43}$
100001 >	12 >	$\lambda_{11}$	111010 >	44 >	$\lambda_{44}$
011000 >	13 >	$\lambda_9$	111001 >	45 >	$\lambda_{44}$
010100 >	14 >	$\lambda_9$	110110 >	46 >	$\lambda_{44}$
010010 >	15 >	$\lambda_{11}$	110101 >	47 >	$\lambda_{44}$
010001 >	16 >	$\lambda_{11}$	110011 >	48 >	$\lambda_{48}$
001100 >	17 >	$\lambda_{17}$	101110 >	49 >	$\lambda_{49}$
001010 >	18 >	$\lambda_9$	101101 >	50 >	$\lambda_{49}$
001001 >	19 >	$\lambda_9$	101011 >	51 >	$\lambda_{44}$
000110 >	20 >	$\lambda_9$	100111 >	52 >	$\lambda_{44}$
000101 >	21 >	$\lambda_9$	011110 >	53 >	$\lambda_{49}$
000011 >	22 >	$\lambda_8$	011101 >	54 >	$\lambda_{49}$
111000 >	23 >	$\lambda_{23}$	011011 >	55 >	$\lambda_{44}$
110100 >	24 >	$\lambda_{23}$	010111 >	56 >	$\lambda_{44}$
110010 >	25 >	$\lambda_{25}$	001111 >	57 >	$\lambda_{43}$
110001 >	26 >	$\lambda_{25}$	111110 >	58 >	$\lambda_{58}$
101100 >	27 >	$\lambda_{27}$	111101 >	59 >	$\lambda_{58}$
101010 >	28 >	$\lambda_{28}$	111011 >	60 >	$\lambda_{60}$
101001 >	29 >	$\lambda_{28}$	110111 >	61 >	$\lambda_{60}$
100110 >	30 >	$\lambda_{28}$	101111 >	62 >	$\lambda_{58}$
100101 >	31 >	$\lambda_{28}$	011111 >	63 >	$\lambda_{58}$
100011 >	32 >	$\lambda_{25}$	111111 >	64 >	$\lambda_{64}$

$$\begin{aligned}
 \lambda_1 &= 0 & \lambda_{27} &= \epsilon_1 + 2\epsilon_2 + 2U + A' - \xi_{27} \\
 \lambda_2 &= \epsilon_1 - \xi_2 & \lambda_{28} &= 2\epsilon_1 + \epsilon_2 + 2U + U' - \xi_{28} \\
 \lambda_4 &= \epsilon_2 - \xi_2 & \lambda_{43} &= 2\epsilon_1 + 2\epsilon_2 + 4U + A + A' - \xi_{43} \\
 \lambda_8 &= 2\epsilon_1 + A - \xi_8 & \lambda_{44} &= 3\epsilon_1 + \epsilon_2 + 3U + 2U' + A - \xi_{44} \\
 \lambda_9 &= 2\epsilon_1 + U' - \xi_9 & \lambda_{48} &= 4\epsilon_1 + 4U' + 2A - \xi_{48} \\
 \lambda_{11} &= 2\epsilon_1 + U' - \xi_{11} & \lambda_{49} &= 2\epsilon_1 + 2\epsilon_2 + 4U + U' + A' - \xi_{49} \\
 \lambda_{17} &= 2\epsilon_2 + A' - \xi_{17} & \lambda_{58} &= 3\epsilon_1 + 2\epsilon_2 + 6U + 2U' + A + A' - \xi_{58} \\
 \lambda_{23} &= 2\epsilon_1 + \epsilon_2 + 2U + A - \xi_{23} & \lambda_{60} &= 4\epsilon_1 + \epsilon_2 + 4U + 4U' + 2A - \xi_{60} \\
 \lambda_{25} &= 3\epsilon_1 + 2U' + A - \xi_{25} & \lambda_{64} &= 4\epsilon_1 + 2\epsilon_2 + 8U + 4U' + 2A + A' - \xi_{64}
 \end{aligned}
 \tag{A.30}$$

$$\xi_p = \sum_{k=1}^2 \frac{1}{2m\omega_k^2} (A_q^{(k)})^2 \quad (\text{A.31})$$

 Appendix 3.  $A_q^{(i)}$  coefficients.

$ q\rangle$	$A_q^{(1)}$	$A_q^{(2)}$	$ q\rangle$	$A_q^{(1)}$	$A_q^{(2)}$	$ q\rangle$	$A_q^{(1)}$	$A_q^{(2)}$
1			23	$A_{23}^{(1)}$	$A_{23}^{(2)}$	45	$A_{44}^{(1)}$	$A_9^{(2)}$
2	$A_2^{(1)}$	$A_2^{(2)}$	24	$A_{23}^{(1)}$	$A_{23}^{(2)}$	46	$A_{44}^{(1)}$	$A_9^{(2)}$
3	$A_2^{(1)}$	$A_2^{(2)}$	25	$A_{25}^{(1)}$	$A_2^{(2)}$	47	$A_{44}^{(1)}$	$A_9^{(2)}$
4	$A_4^{(1)}$		26	$A_{25}^{(1)}$	$A_2^{(2)}$	48	$A_{48}^{(1)}$	
5	$A_4^{(1)}$		27	$A_{27}^{(1)}$	$A_{27}^{(2)}$	49	$A_{49}^{(1)}$	
6	$A_2^{(1)}$	$-A_2^{(2)}$	28	$A_{28}^{(1)}$		50	$A_{49}^{(1)}$	
7	$A_2^{(1)}$	$-A_2^{(2)}$	29	$A_{28}^{(1)}$		51	$A_{44}^{(1)}$	$-A_9^{(2)}$
8	$A_8^{(1)}$	$A_8^{(2)}$	30	$A_{28}^{(1)}$		52	$A_{44}^{(1)}$	$-A_9^{(2)}$
9	$A_9^{(1)}$	$A_9^{(2)}$	31	$A_{28}^{(1)}$		53	$A_{49}^{(1)}$	
10	$A_9^{(1)}$	$A_9^{(2)}$	32	$A_{25}^{(1)}$	$-A_2^{(2)}$	54	$A_{49}^{(1)}$	
11	$A_{11}^{(1)}$		33	$A_{27}^{(1)}$	$A_{27}^{(2)}$	55	$A_{44}^{(1)}$	$-A_9^{(2)}$
12	$A_{11}^{(1)}$		34	$A_{28}^{(1)}$		56	$A_{44}^{(1)}$	$-A_9^{(2)}$
13	$A_9^{(1)}$	$A_9^{(2)}$	35	$A_{28}^{(1)}$		57	$A_{43}^{(1)}$	$-A_{43}^{(2)}$
14	$A_9^{(1)}$	$A_9^{(2)}$	36	$A_{28}^{(1)}$		58	$A_{58}^{(1)}$	$A_{27}^{(2)}$
15	$A_{11}^{(1)}$		37	$A_{28}^{(1)}$		59	$A_{58}^{(1)}$	$A_{27}^{(2)}$
16	$A_{11}^{(1)}$		38	$A_{25}^{(1)}$	$-A_2^{(2)}$	60	$A_{60}^{(1)}$	
17	$A_{17}^{(1)}$		39	$A_{27}^{(1)}$	$-A_{27}^{(2)}$	61	$A_{60}^{(1)}$	
18	$A_9^{(1)}$	$-A_9^{(2)}$	40	$A_{27}^{(1)}$	$-A_{27}^{(2)}$	62	$A_{58}^{(1)}$	$-A_{27}^{(2)}$
19	$A_9^{(1)}$	$-A_9^{(2)}$	41	$A_{23}^{(1)}$	$-A_{23}^{(2)}$	63	$A_{58}^{(1)}$	$-A_{27}^{(2)}$
20	$A_9^{(1)}$	$-A_9^{(2)}$	42	$A_{23}^{(1)}$	$-A_{23}^{(2)}$	64	$A_{64}^{(1)}$	
21	$A_9^{(1)}$	$-A_9^{(2)}$	43	$A_{43}^{(1)}$	$A_{43}^{(2)}$			
22	$A_8^{(1)}$	$-A_8^{(2)}$	44	$A_{44}^{(1)}$	$A_9^{(2)}$			

$$A_2^{(1)} = \frac{1}{\sqrt{2}}\bar{\gamma}$$

$$A_{28}^{(1)} = \sqrt{2}(\bar{\gamma} - \gamma' + \bar{\alpha} + \bar{\beta})$$

$$A_4^{(1)} = -\sqrt{2}\gamma'$$

$$A_{43}^{(1)} = \sqrt{2}(\bar{\gamma} - 2\gamma' + 2\bar{\alpha})$$

$$A_8^{(1)} = \sqrt{2}\bar{\gamma}$$

$$A_{44}^{(1)} = \frac{1}{\sqrt{2}}(3\bar{\gamma} - 2\gamma' + 3\bar{\alpha} + 4\bar{\beta})$$

$$A_9^{(1)} = \frac{1}{\sqrt{2}}\bar{\gamma} - \sqrt{2}\gamma' + \frac{1}{\sqrt{2}}\bar{\alpha}$$

$$A_{48}^{(1)} = 2\sqrt{2}(\bar{\gamma} + 2\bar{\beta})$$

$$A_{11}^{(1)} = \sqrt{2}(\bar{\gamma} + \bar{\beta})$$

$$A_{49}^{(1)} = \sqrt{2}(\bar{\gamma} - 2\gamma' + 4\bar{\alpha} + 2\bar{\beta})$$

$$A_{17}^{(1)} = -2\sqrt{2}\gamma'$$

$$A_{58}^{(1)} = \frac{1}{\sqrt{2}}(3\bar{\gamma} - 4\gamma' + 6\bar{\alpha} + 4\bar{\beta})$$

$$A_{23}^{(1)} = \sqrt{2}(\bar{\gamma} - \gamma' + \bar{\alpha})$$

$$A_{60}^{(1)} = \sqrt{2}(2\bar{\gamma} - \gamma' + 2\bar{\alpha} + 4\bar{\beta})$$

$$A_{25}^{(1)} = \frac{3}{\sqrt{2}}\bar{\gamma} + 2\sqrt{2}\bar{\beta}$$

$$A_{64}^{(1)} = 2\sqrt{2}(\bar{\gamma} - \gamma' + 2\bar{\alpha} + 2\bar{\beta})$$

$$A_{27}^{(1)} = \frac{1}{\sqrt{2}}(\bar{\gamma} - 4\gamma' + 2\bar{\alpha})$$

$$A_2^{(2)} = -\gamma\sqrt{\frac{M}{2m'}} \quad A_{23}^{(2)} = -2(\gamma + \bar{\alpha})\sqrt{\frac{M}{2m'}}$$

$$A_8^{(2)} = -2\gamma\sqrt{\frac{M}{2m'}} \quad A_{27}^{(2)} = -(\gamma + 2\bar{\alpha})\sqrt{\frac{M}{2m'}}$$

$$A_9^{(2)} = -(\gamma + \bar{\alpha})\sqrt{\frac{M}{2m'}} \quad A_{43}^{(2)} = -2(\gamma + 2\bar{\alpha})\sqrt{\frac{M}{2m'}}$$

### Acknowledgements

This work was partially supported by State Committee of Science and Technology of Ukraine, Grant No 2.3/806.

The research described in the publication was made possible in part by Grant No K6A100 from the Joint Fund of the Government of Ukraine and International Science Foundation.

### References

- [1] Ranninger R. On the lattice properties and electron-lattice interaction in high- $T_c$  superconductors. // *Z. Phys. B.*, 1991, vol. 84, p. 167-178.
- [2] Gervais V. Oxygen polarizability in ferroelectrics. a clue to understanding superconductivity in oxides? // *Ferroelectrics*, 1992, vol. 130, p. 117-128.
- [3] Mustre de Leon J., Conradson S. D., Batistic I., and Bishop A. R. Correlations between axial-oxygen anharmonicity and  $T_c$  in  $YBa_2Cu_3O_7$  and related compounds. // *Phys. Rev. B.*, 1991, vol. 44, p.2422-2425.
- [4] Janoschek R., Weidemann E. G. and Zundel G. Calculation frequencies and intensities associated with coupling of the proton motion with the hydrogen bond stretching vibration in a double minimum potential surface. // *Journ. of the Amer. Chem. Soc.*, 1973, vol. 69, p. 505.
- [5] Mackowiak M. NQR study of high pressure deformation of the hydrogen bond potential. // *Journ. Mol. Structure*, 1989, vol. 192, p. 189-198.
- [6] Scheiner S. // *Proton transfer in hydrogen-bonded systems.* / Eds. by T.Bountis, Plenum Press, N.Y., 1992, p. 29-47
- [7] Mustre de Leon J., Batistic I., Bishop A. R., Conradson S. D. and Trugman S. A. A Polaron origin for the anharmonicity of the axial oxygen in  $YBa_2Cu_3O_7$  crystal. // *Phys. Rev. Lett.*, 1992, vol. 68, p. 3236-3239.
- [8] Holstein T. // *Annals of Physics (N.Y.)*, 1959, vol. 8, p. 325-343.
- [9] Zhong J., Schüttler H.-B. Polaron anharmonicity in the holstein-hubbard model. // *Phys. Rev. Letters*, 1992, vol. 69, p. 1600-1603.
- [10] Konior J. Anharmonic-polaronic model and high- $T_c$  superconductivity. // *Phys. Rev. B.*, 1993, vol. 47, p. 14425-14433.
- [11] Inada Y. Effective interaction between electrons due to exchange of breathing phonons in High- $T_c$  superconducting oxides. // *Journ. Phys. Soc. Japan*, 1990, vol. 59, p. 2295-2296.
- [12] Das A. N., Sil S. Electron-phonon interaction in a strongly correlated hubbard system. // *Physica C*, 1989, vol. 161, p. 325-330.
- [13] Stasyuk I. V. and Sizonenko Yu. V. Adiabatic potentials of quasi-one-dimensional systems with local anharmonicities. , Lviv, 1993, Prepr./Acad. Sci. Ukr., Inst. Cond. Matt. Phys. ICMP-93-26U, (in Ukrainian).
- [14] Shüttler H.-B. et al. // *J.Low.Temp.Phys.*, 1987, vol. 69, p.159

- [15] Shütler H.-B. and Fedro A. J. Effective strong coupling hamiltonians for bipolaron centers and magnetic impurities with on-site electron coupling. // Phys. Rev. B., 1988, vol. 38, p. 9063-9068.
- [16] Lang L. G. and Firsow Yu. A. Kinetic theory of semiconductors with a low mobility. // Zh. Eksp. Teor. Fiz., 1962, vol. 43, p. 1843-1860, (in Russian).
- [17] Müller K. A. Phase Transitions (special issue).
- [18] Frick M., von der Linden W., Morgenstern I. and de Raedt H. Local anharmonic vibrations, strong correlations and superconductivity. // Z. Phys. B., 1990, vol. 81, p. 327-335.
- [19] Stasyuk I. V. and Shvaika A. M. Dielectric instability and local anharmonic model in the theory of high- $T_c$  superconductivity. // Physica C, 1994, vol. 235-240, p. 2173-2174.
- [20] Klimontovich Yu. L. Statistical Physics, Moscow, Nauka, 1982, 606 p., (in Russian).

## ЕФЕКТИВНІ ЛОКАЛЬНІ АДІАБАТИЧНІ ПОТЕНЦІАЛИ В ТВЕРДИХ ТІЛАХ. МОДЕЛЬНИЙ ПІДХІД

І.В. Стасюк, Ю.В. Сизоненко

На основі простої моделі досліджується роль електрон-фононної взаємодії в утворенні локальних ангармонічних потенціалів ґратки. На прикладі 3-іонного кластера  $A-B-A$  розглядається взаємодія електронної підсистеми з коливними модами  $u_r$  та  $u_{ir}$ , які є КР- та ІЧ-активні відповідно. Розраховуються ефективні іонні потенціали та функції розподілу. Проаналізовано можливість появи одного  $(u_r^0, 0)$  або двох  $(u_r^0, \pm u_{ir}^0)$  рівноважних положень кластера при різних значеннях параметрів моделі. Побудовано фазові діаграми для характеристики різних можливих станів кластера та, відповідно, різних топологічних типів ефективних потенціалів. Досліджується енергетичний спектр моделі. Показано, що квазіполяронний ефект приводить до утворення дублету в низькочастотній ділянці спектру. Віддаль між його підрівнями визначається параметром електронного переносу, перенормованого за рахунок електрон-фононної взаємодії.